ANL-ART-194

Preliminary description of a new creep-fatigue design method that reduces over conservatism and simplifies the high temperature design process

Applied Materials Division

ANL-ART-194

Preliminary description of a new creep-fatigue design method that reduces over conservatism and simplifies the high temperature design process

Applied Materials Division
Argonne National Laboratory

September 2020

Prepared by

B. Barua, Argonne National Laboratory

M. C. Messner, Argonne National Laboratory

T. –L. Sham, Argonne National Laboratory

R. I. Jetter, RI Jetter Consulting

Y. Wang, Oak Ridge National Laboratory

ABSTRACT

The report provides the initial description of a new creep-fatigue design method for structural components in high temperature nuclear service. The new method is based on an integrated elastic-perfectly plastic (EPP) analysis and Simplified Model Test (SMT) approach that reduces over conservatism, improves the treatment of elastic follow up, and simplifies the design procedure, when compared with the current creep-fatigue design methods in ASME Boiler and Pressure Vessel Code. Developing the design charts for the EPP-SMT design method requires extrapolating SMT test data as a function of hold time and follow up factor. The report develops the preliminary design charts for Alloy 617 at temperatures between 800°C and 950°C by combining two extrapolation approaches developed in a previous work. The report also presents a comparative analysis between the EPP-SMT design method and the current ASME creep-fatigue design methods by evaluating design life of two sample geometries under different loading conditions. Results from the comparative analysis verify the EPP-SMT design charts but suggest the requirement of additional test data in the low strain range regime for improving the extrapolation procedure that will further reduce the over conservatism in the creep-fatigue damage evaluation. The report also concludes that the EPP-SMT design procedure can account for effect of primary load on creep-fatigue life by using a fixed, bounding value of follow up in constructing the design charts. The conclusions to this report describe the future work required to complete this new design method so it can be codified through a nuclear Code Case

TABLE OF CONTENTS

LIST OF FIGURES

LIST OF TABLES

1 Introduction

Currently, the ASME Boiler and Pressure Vessel Code includes three creep-fatigue design methods – design by elastic analysis and design by inelastic analysis in Section III, Division 5 [1] and design by elastic-perfectly plastic (EPP) analysis in Code Case N-862 [2] – for high temperature nuclear structural components. All three methods use the same fundamental approach for assessing the creep-fatigue damage. The approach requires calculating creep and fatigue damages separately and then comparing those with the damage interaction diagram, also known as D-diagram, to assess the interaction of creep and fatigue. However, this approach is empirical and suffers from over conservatism. Moreover, the design by elastic and design by elastic-perfectly plastic analysis methods treat elastic follow up in an approximate, bounding, but very conservative way and therefore may overestimate the detrimental effect of follow up on creep-fatigue life. Furthermore, the overall procedure for creep-fatigue damage evaluation in current design methods has been perceived as complicated and difficult to execute. For example, calculating creep damage in design by elastic analysis method requires constructing the relaxation profile through a complicated series of rules designed to account for plasticity and creep in an otherwise linear elastic solution.

This report provides the preliminary description of an improved new creep-fatigue design method that reduces over conservatism, accounts for elastic follow up more accurately, and is easier to execute. This new design method is based on an approach that combines the EPP analysis approach and design allowable curves, conceptually, from Simplified Model Test (SMT) specimens [3]. The EPP analysis approach greatly simplifies the design evaluation procedure in several ways. It allows a designer to bound all the complicated material effects using a simple constitutive model. The effective strain range estimated through EPP analysis at any point of the structure approximately accounts for creep and plasticity [4]. This eliminates the need for stress classification used in the design by elastic analysis method to account for creep and plasticity. Moreover, the EPP analysis approach uses the steady cyclic effective strain range from a shakedown analysis. This means a designer only needs to simulate the component for a handful number of cycle repetitions instead of simulating for the complete load history. Furthermore, the EPP analysis approach does not require or store the material state and therefore allows analyzing each individual load cycle separately and afterwards superimposing results. This is beneficial from a practical design viewpoint, as changing the definition of a single load will not require reanalyzing the component for the entire load history.

The second aspect of the EPP-SMT design method is the use of SMT data to establish the design allowable curves. The SMT specimen, developed through extensive research and development work [5][6][7][8][9][23][24][25][26], can directly assess the effect of elastic follow up on cyclic creep-fatigue life. This data avoids the use of D-diagram for creep-fatigue evaluation while accurately accounting for elastic follow up arising from localized defect and stress risers. Elastic follow up is described in detail in [10][24].

Several elements of the EPP-SMT design method were developed in past years with support from the Advanced Reactor Technologies (ART) program and are summarized in three Argonne National Laboratory (ANL) technical reports [10][11][12]. [10] describes a simple version of the design method for one type of loading cycle and for uniaxial deformation. [11] extends this basic methodology to account for multiaxial loading and the effect of combined load cycles. This report

discusses several methods based on the Huddleston model [13] for calculating the effective strain range from EPP analysis. Although a final recommendation on the effective strain range measure must await the development of multiaxial SMT test, until then, the report recommends retaining the current ASME definition of effective strain range. The report also explored several techniques for combining load cycles before recommending a new definition of composite cycle for the EPP-SMT design method, modified from the composite cycle definition used in design by elastic-perfectly plastic analysis. [12] develops the definition of the pseudoyield stress for the EPP analysis to determine the stable cyclic strain range. The report presents several validation examples demonstrating the effectiveness of the analysis method in representing strain ranges in simple experimental tests and also in more complex, realistic structural components. Another element of the design method development is it should capture the primary load effect on creep-fatigue damage, as primary loads cause stresses in the component that creep stress relaxation cannot diminish. Chapter 4 of this report discusses this aspect of the EPP-SMT design method development.

Finally, the completion of the EPP-SMT design method requires the development of the design allowable curves. Chapter 2 develops the preliminary design charts for creep-fatigue damage evaluation in the EPP-SMT design methodology through examining the approaches developed in [10] for extrapolating creep-fatigue and SMT test data at high strain ranges with short holds to low strain ranges with long holds, as typical of structural components in high temperature nuclear service. Chapter 3 verifies the approach used in constructing preliminary design charts via comparative analysis between EPP-SMT design method and current ASME design methods for two sample structures. Chapter 5 provides the initial version of the EPP-SMT design method. Chapter 6 summarizes the conclusions developed here and describes the future work required to complete the EPP-SMT design method and codify it through an ASME nuclear Code Case.

2 Development of EPP-SMT design charts

The EPP-SMT design method requires allowable design charts to be used as the acceptance criteria for creep-fatigue damage evaluation. These design charts are essentially modified fatigue curves plotting an effective strain range versus the number of cycles to failure. In addition to the effect of strain range and temperature, as in the conventional fatigue design curves, the EPP-SMT design curves must account for the effect of hold time and elastic follow up. The SMT test methodology was developed to experimentally control all four variables. However, like the conventional creep-fatigue tests, performing the SMT tests at low strain ranges with long holds, typical for structural components under operating conditions, is not practically possible. Although both types of tests are conceptually possible, they would take very long time to complete. Moreover, since the EPP-SMT approach has recently been developed, the current SMT experimental database is limited compared to the historical creep-fatigue tests.

To develop EPP-SMT curves from limited creep-fatigue and SMT test data two approaches – (a) direct extrapolation and (b) classical approach – have been proposed in a previous report [10]. Note the change in terminology from the previous work: there we used Option-A and Option-B, here we use direct extrapolation and classical approach. The terms are used synonymously. Both approaches use a modified Coffin-shift model for extrapolating the creep-fatigue and SMT test data with short hold times to long hold times expected in operating components. This chapter develops EPP-SMT curves using both approaches and makes recommendations on the approach to use for developing design charts. The recommended approach is verified in Chapter 3 by comparing the EPP-SMT design method with other design methods in ASME Code for two structural components, subjected to different thermal and pressure loading conditions.

2.1 Modified Coffin-shift model

The base Coffin-shift model originates from the frequency-modified fatigue equations proposed by Coffin [14] for time-dependent fatigue. It is essentially the standard $N = \frac{C}{\Delta\varepsilon}$ equation for the fatigue curve multiplied with a factor to account for the hold time:

$$N = \frac{C}{\Delta\varepsilon}\left(\frac{1}{1+t_h}\right)^p \tag{2.1}$$

where N is the cycles to failure, $\Delta\varepsilon$ is the strain range, t_h is the hold time, and C and p are some constants. C can be determined from fatigue test data, while p can be determined from creep-fatigue test data. Although not used in the current ASME Code, this approach of modifying fatigue curves to account for hold time effect was used in previous versions of the Code [10].

Previous work [10] demonstrated that the base Coffin-shift model exaggerates the effect of hold time on cyclic life when compared with Alloy 617 creep-fatigue experimental data at 950°C. Fundamentally, stress in the material relaxes under creep-fatigue loading and for a long enough hold time will reach to a point where it accumulates negligible creep damage. The saturation of the creep damage accumulation with the increase of hold time is not reflected in the base Coffin-shift model as the model postulates zero cyclic life for an infinite hold time. Therefore, to capture the

saturation of creep damage accumulation with increasing hold time, the base Coffin-shift model was modified to:

$$N = \frac{C}{\Delta\varepsilon}\frac{(\frac{1}{1+t_h})^p + D}{1+D} \tag{2.2}$$

where D is a constant and can be determined from creep-fatigue test data. This model was found to reasonably capture the trend of creep-fatigue experimental data reported in [10] for Alloy 617 at 950°C. Assuming some general inverse power dependence of the cyclic life on elastic follow up Equation 2.2 can be modified to:

$$N = \frac{1}{q^a}\frac{C}{\Delta\varepsilon}\frac{(\frac{1}{1+t_h})^p + D}{1+D} \tag{2.3}$$

to include the effect of elastic follow up on the cyclic life. In Equation 2.3, q is the follow up factor and exponent a can be determined by fitting the SMT test data. Based on the analysis done in the previous work [10], the value of a was found to be approximately 1.0 which reduces Equation 2.3 to:

$$N = \frac{1}{q}\frac{C}{\Delta\varepsilon}\frac{(\frac{1}{1+t_h})^p + D}{1+D} \tag{2.4}$$

Equation 2.4 can be regarded as the final modified Coffin-shift model for EPP-SMT curves which captures the combined effect of hold time, elastic follow up, and strain range on the cyclic life. This model is interesting as the effect of individual parameters can be easily separated. For $q = 1$ and $t_h = 0$, the model describes the correlation between the strain range and cyclic life in fatigue tests. When $q = 1$ and $t_h > 0$, the model represents material behavior under creep-fatigue loading. Then, with $q > 1$ the model captures the effect of elastic follow up. Therefore, $\frac{1}{q}\frac{(\frac{1}{1+t_h})^p + D}{1+D}$ in Equation 2.4 can be regarded as the shift factor to fatigue curves for the combined effect of the hold and elastic follow up. Since q is fixed in SMT tests, the constants p and D can be considered as shift parameters which can be determined either from creep-fatigue tests, as stated above, or from combined data sets of creep-fatigue tests and SMT tests with holds. We used the former while the SMT test data were used for verification purpose only.

Figure 2.1 to Figure 2.3 show the modified Coffin-shift model fit to the fatigue and creep-fatigue experimental data for Alloy 617 at temperatures 800°C, 850°C, and 950°C, respectively. Since these data are from fatigue and creep-fatigue tests, the value of q is 1.0. Note the model fails to capture the test results for low strain ranges and therefore only test data in the high strain range regime were used for these calibrations. Since the model assumes a linear correlation between $logN$ and $log\Delta\varepsilon$, it only captures the low cycle regime of the fatigue data which usually follow a linear trend in $logN - log\Delta\varepsilon$ space. Table 2.1 lists the best-fit parameters for all three temperatures.

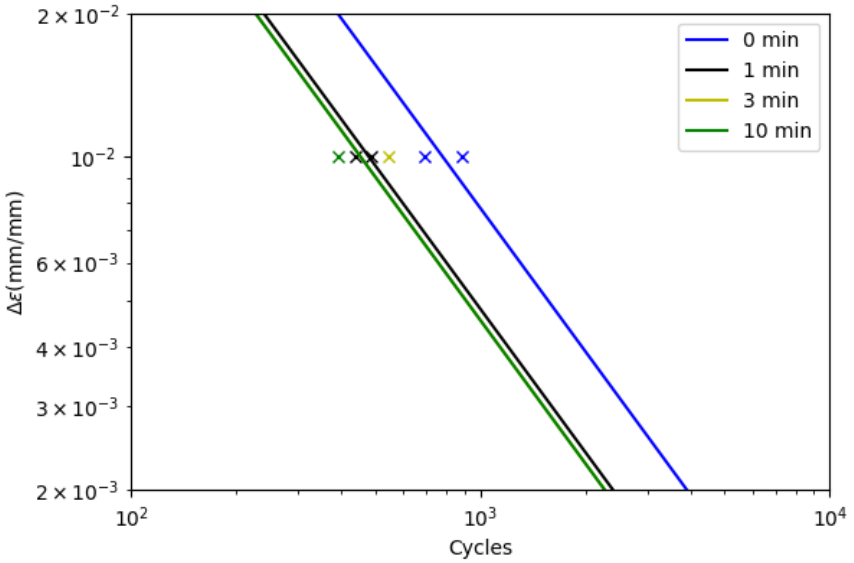

Figure 2.1: Curve fit to the experimental fatigue and creep-fatigue data of Alloy 617 at 800°C using the modified Coffin-shift model (Equation 2.4). The follow up factor, q is 1.0 for fatigue and creep-fatigue test.

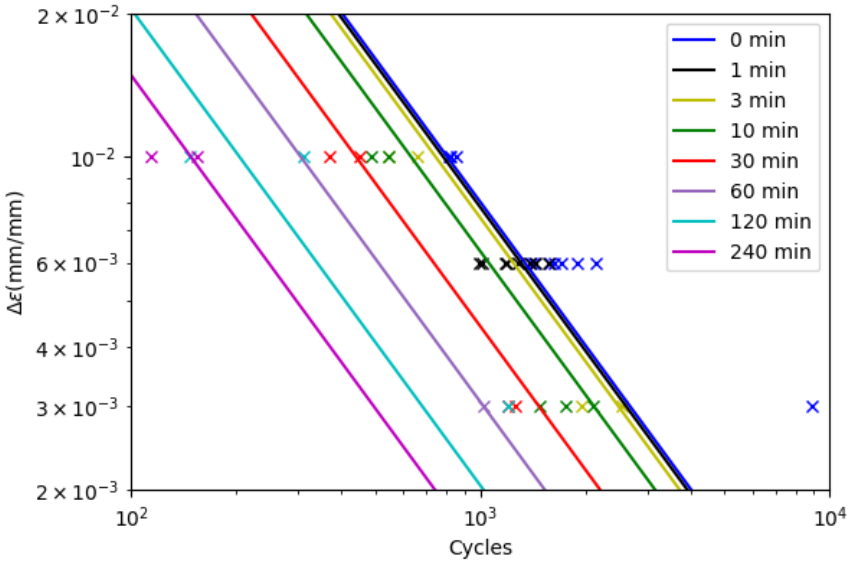

Figure 2.2: Curve fit to the experimental fatigue and creep-fatigue data of Alloy 617 at 850°C using the modified Coffin-shift model (Equation 2.4). The follow up factor, q is 1.0 for fatigue and creep-fatigue test.

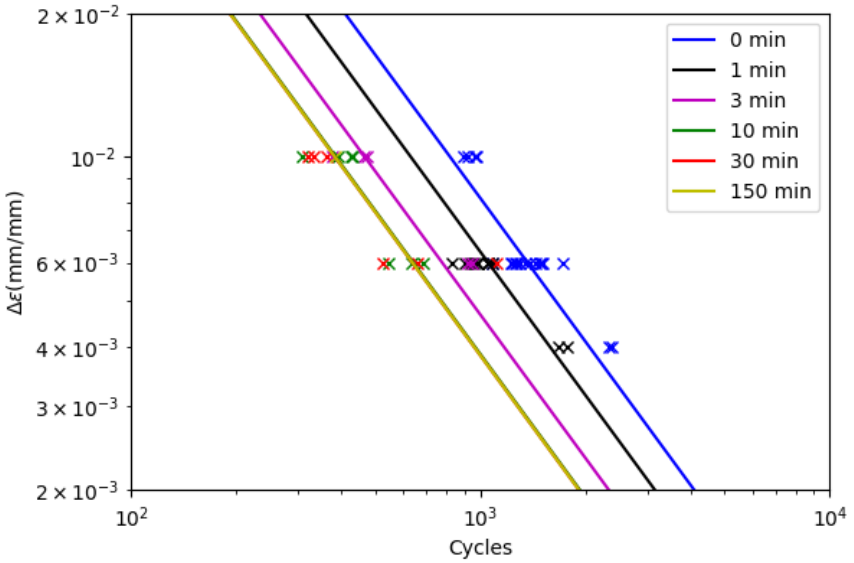

Figure 2.3: Curve fit to the experimental fatigue and creep-fatigue data of Alloy 617 at 950°C using the modified Coffin-shift model (Equation 2.4). The follow up factor, q is 1.0 for fatigue and creep-fatigue test.

Temperature (°C)	C	p	D
800	7.80	154.38	1.39
850	8.04	1.84	0.16
950	8.18	33.9	0.88

Table 2.1: Parameters for the modified Coffin-shift model for Alloy 617 at different temperatures.

2.2 Extrapolation approaches

As described above, generating a creep-fatigue and SMT test database at low strain ranges and long holds is practically impossible. Therefore, a method must be developed for extrapolating the test data at high strain ranges and short hold times to the low strain ranges and long hold times that are typically experienced by the structural components in high temperature nuclear service. Two approaches for developing such a method are discussed below.

2.2.1 Direct extrapolation

This approach directly extrapolates the results of creep-fatigue and SMT tests data using the modified Coffin-shift model. Essentially, it uses the parameters listed in Table 2.1 and Equation 2.4 to determine the cycles to failure at a given strain range, hold time, and follow up factor. A schematic describing this approach along with the classical approach, as discussed below, is shown in Figure 2.4. The creep-fatigue trendline is first determined using high strain range, short hold test data which is then extrapolated to realistic long hold times and low strain range regime. For the direct extrapolation approach of the EPP-SMT curves Equation 2.4 can be rewritten as:

$$N_{SMT,nominal}^{Direct} = \frac{1}{q}\frac{C}{\Delta\varepsilon}\frac{(\frac{1}{1+t_h})^p+D}{1+D} \quad (2.5)$$

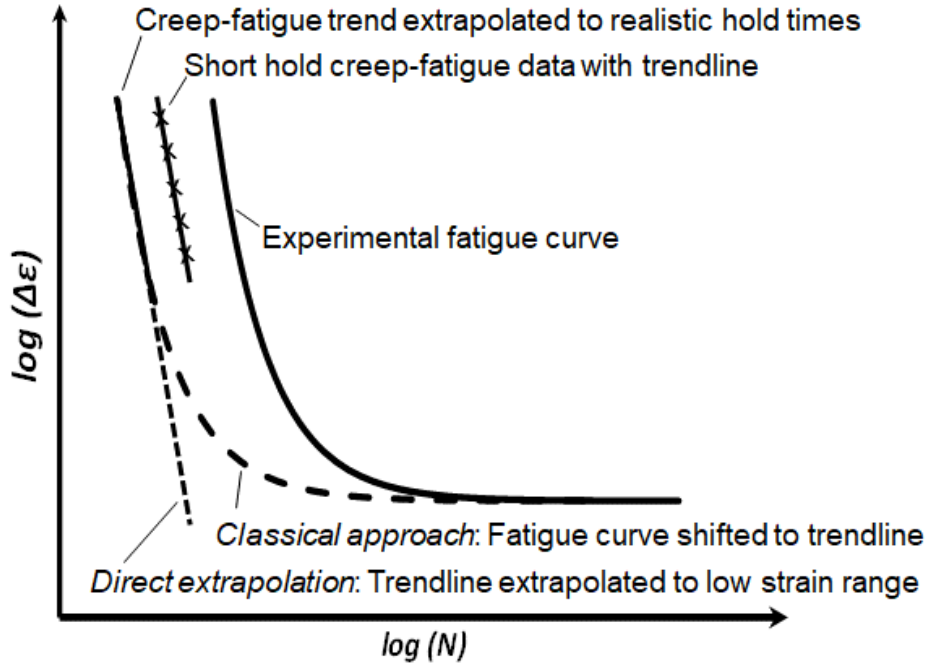

Figure 2.4: Schematic demonstrating two different approaches for extrapolating high strain range, short hold time experimental data to low strain range, long hold time.

2.2.2 Classical approach

Since the standard fatigue equation $N = \frac{C}{\Delta\varepsilon}$, that is used in the Coffin-shift model, cannot capture the behavior of the material in low strain range regime, an alternate approach to the direct extrapolation of the test data could be shifting the experimental fatigue curve. This approach can be called classical approach. It is still based on the Coffin-shift approach but shifts the nominal fatigue curve instead of the trendline determined using high strain range data. Therefore, for classical approach Equation 2.4 can be modified to:

$$N_{SMT,nominal}^{Classical} = N_{fatigue,nominal}\left\{\frac{1}{q}\frac{(\frac{1}{1+t_h})^p+D}{1+D}\right\} \quad (2.6)$$

where $N_{fatigue,nominal}$ represents the nominal fatigue curve. The shift factor is determined using the parameters p and D from Table 2.1 and follow up factor q. An illustration of this approach is sketched in Figure 2.4. As shown in the figure, the nominal fatigue curve is shifted to the realistic long hold time based on the shift factor predicted by Equation 2.4. In this approach, an accurate

representation of the high cycle fatigue life is combined with a good accounting of the effect of hold time and elastic follow up to determine the EPP-SMT life.

2.3 EPP-SMT curves

Two approaches are discussed above for constructing EPP-SMT curves through extrapolating the test data with short hold times. This section compares the EPP-SMT curves from both approaches with test data. The creep-fatigue test data are first compared with nominal EPP-SMT curves with no elastic follow up (i.e. $q = 1$). SMT test data with different elastic follow ups are then compared with nominal EPP-SMT curves. Based on these comparisons this section makes recommendations for developing preliminary EPP-SMT design curves. More test data are required before finalizing the design curves but Chapter 3 addresses the verification of the preliminary design curves.

2.3.1 Comparison with creep-fatigue tests

Figure 2.5 to Figure 2.19 plot the nominal EPP-SMT curves, based on the two approaches discussed above, for Alloy 617 at different temperatures and hold times. To compare with the creep-fatigue test data the effect of elastic follow up was not considered, i.e. $q = 1$ in Equations 2.5 and 2.6. These figures also plot the nominal fatigue curve along with fatigue test data. The nominal fatigue curve was constructed from the design fatigue chart provided in Alloy 617 Code Case [15]. Since the Code applies a margin of 2 on the strain range and 20 on cycles to failure in fatigue test data to construct the design fatigue chart, we back calculated the nominal fatigue curve from the design fatigue chart using:

$$\Delta\varepsilon_{nominal}(N) = \max\left\{2 * \Delta\varepsilon_{design}(N),\ \Delta\varepsilon_{design}\left(\frac{N}{20}\right)\right\} \tag{2.7}$$

Figure 2.5 to Figure 2.19 indicate the reconstructed nominal fatigue curves closely match with the fatigue test data. For each temperature and hold time combination, as in each figure, two EPP-SMT curves are plotted – one based on the direct extrapolation approach and the other based on the classical approach. Since the classical approach only shifts the fatigue curve, the shape of the EPP-SMT curve in this approach follows the shape of the fatigue curve. While the EPP-SMT curves based on the direct extrapolation approach follows a linear relationship – essentially obtained from the high strain range data – between $log\Delta\varepsilon$ and $logN$.

The comparison between the EPP-SMT curves and the experimental data indicates that both approaches predict the experimental results for most of the cases when the strain range is about 1%. However, with the decrease of strain range the direct extrapolation approach seems to under predict the cyclic life determined from creep-fatigue test, at least for a few cases. In contrast, the classical approach appears to over predict the cyclic life with the decrease of strain range. Note the creep-fatigue experimental data are only available for a strain range equal to 0.3% or higher. Therefore, a direct comparison could not be made for low strain range regime.

The plots in Figure 2.5 to Figure 2.19 also indicate a significant variation in cyclic life between two approaches in the low strain range regime. For example, under a creep-fatigue loading of 0.15% strain range and 10 minutes hold at 850°C the direct extrapolation approach predicts cyclic life of $5.4\text{x}10^3$ cycles for Alloy 617 compared to $1.0\text{x}10^7$ cycles predicted by the classical approach. Direct testing to determine which of the two approaches reasonably predicts the life in the low strain range regime is practically impossible as the high cycle creep-fatigue test even with

short hold time will take a very long time to complete. An alternate testing approach could be performing SMT tests with large elastic follow up factor. According to Equation 2.4 the cyclic life varies inversely with the follow up factor. Therefore, the test time could be reduced to some extent by using large value of q. One such SMT test data with a 3 minute hold time is available for Alloy 617. The SMT test data is compared with the predicted nominal curves in Section 2.3.2.

Even when generating more SMT test data at low strain ranges direct verification of the extrapolation procedure is only possible for short hold times. SMT tests with long holds are still going to take years to complete and therefore are practically impossible. An alternative, albeit indirect, approach could be comparing the EPP-SMT design method with the current creep-fatigue design methods in the ASME Code. This involves creep-fatigue life evaluation of structures – covering both simple and complex representative reactor components – subjected to different pressure and thermal loadings with a hold time typical of reactor operating condition. Depending on the approach used in generating the EPP-SMT design curves, the EPP-SMT design method will estimate different creep-fatigue lives of the structure. Therefore, by comparing with the creep-fatigue life estimated by other design methods the extrapolation approach for the EPP-SMT curves can be verified. The verification of extrapolation approach through structural component analyses is discussed in Chapter 3.

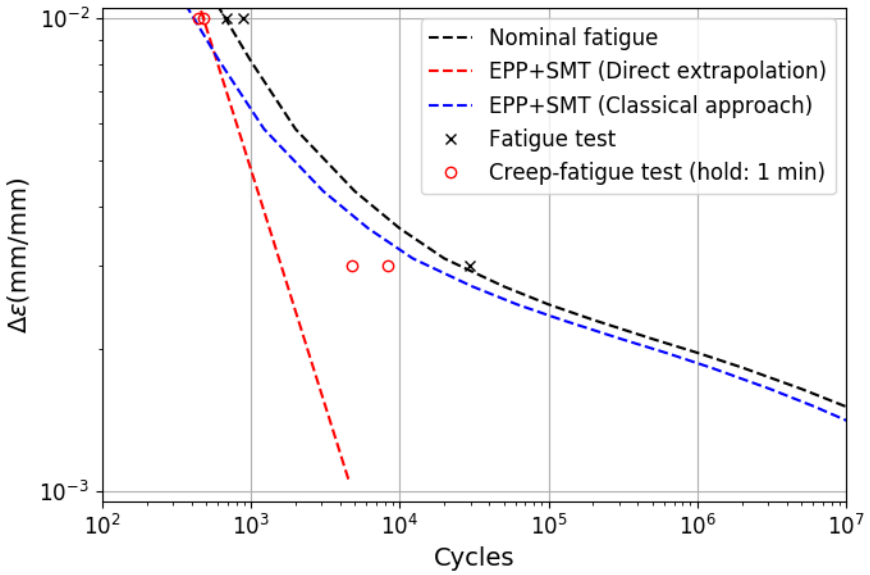

Figure 2.5: Nominal EPP-SMT curves compared with creep-fatigue (i.e. $q = 1$) experimental data for Alloy 617 at 800°C with 1 min hold.

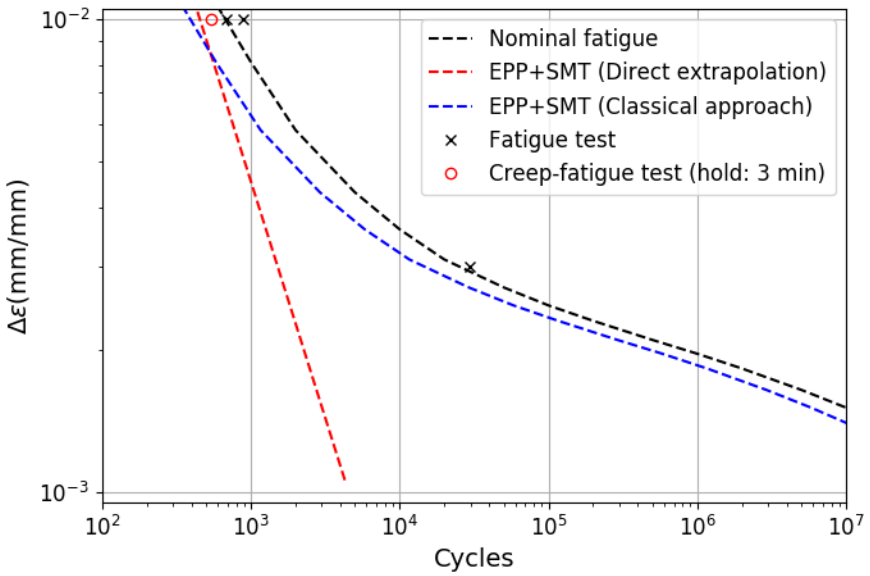

Figure 2.6: Nominal EPP-SMT curves compared with creep-fatigue (i.e. $q = 1$) experimental data for Alloy 617 at 800°C with 3 min hold.

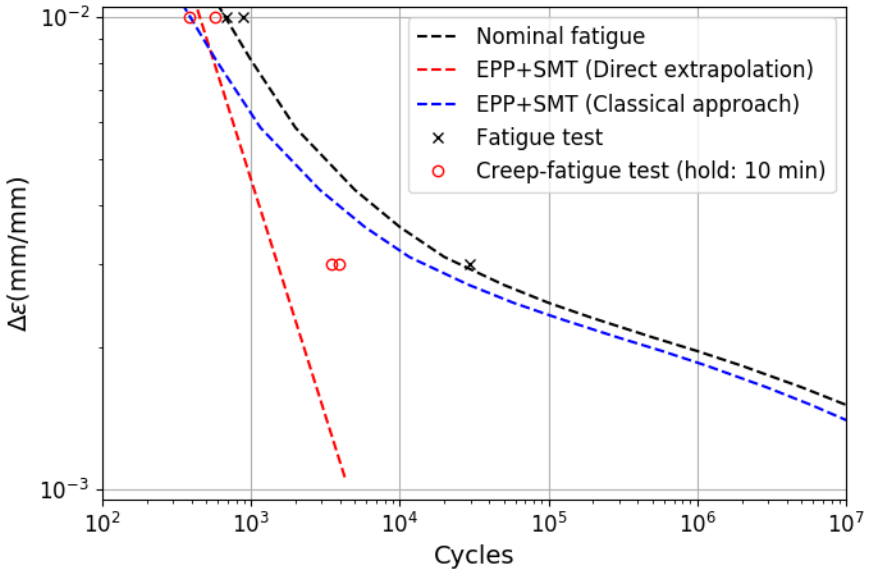

Figure 2.7: Nominal EPP-SMT curves compared with creep-fatigue (i.e. $q = 1$) experimental data for Alloy 617 at 800°C with 10 min hold.

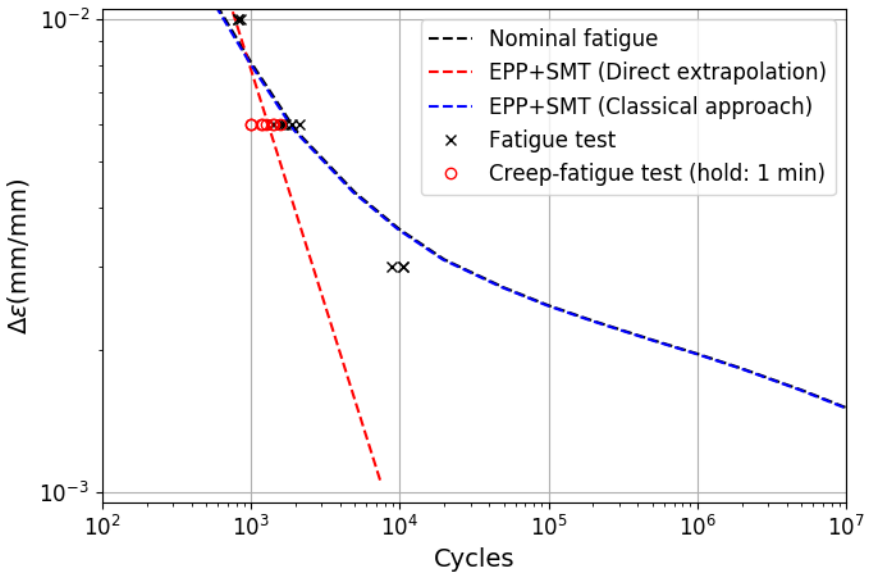

Figure 2.8: Nominal EPP-SMT curves compared with creep-fatigue (i.e. $q = 1$) experimental data for Alloy 617 at 850°C with 1 min hold.

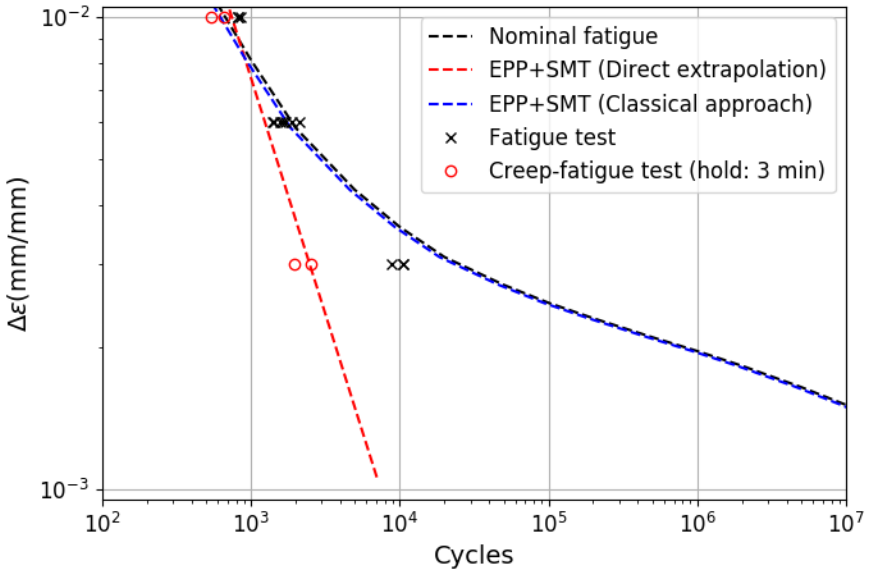

Figure 2.9: Nominal EPP-SMT curves compared with creep-fatigue (i.e. $q = 1$) experimental data for Alloy 617 at 850°C with 3 min hold.

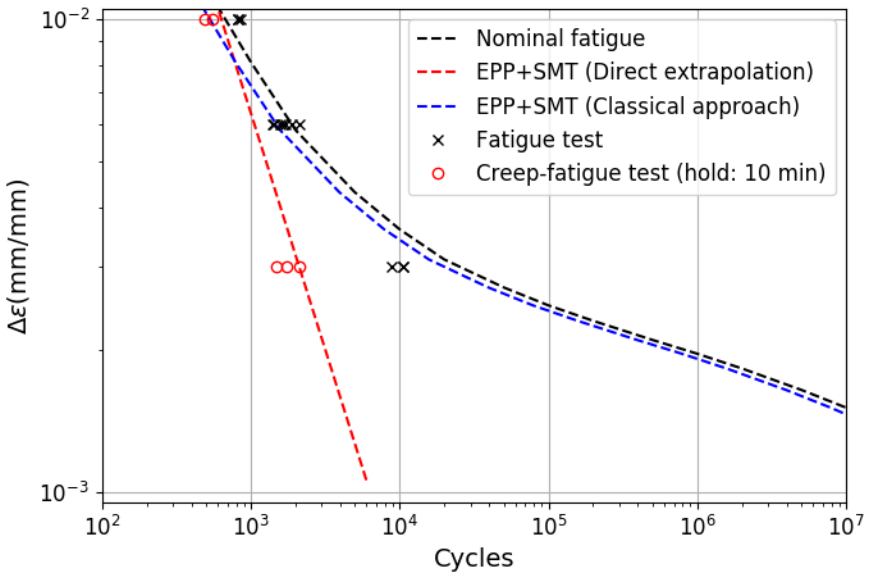

Figure 2.10: Nominal EPP-SMT curves compared with creep-fatigue (i.e. $q = 1$) experimental data for Alloy 617 at 850°C with 10 min hold.

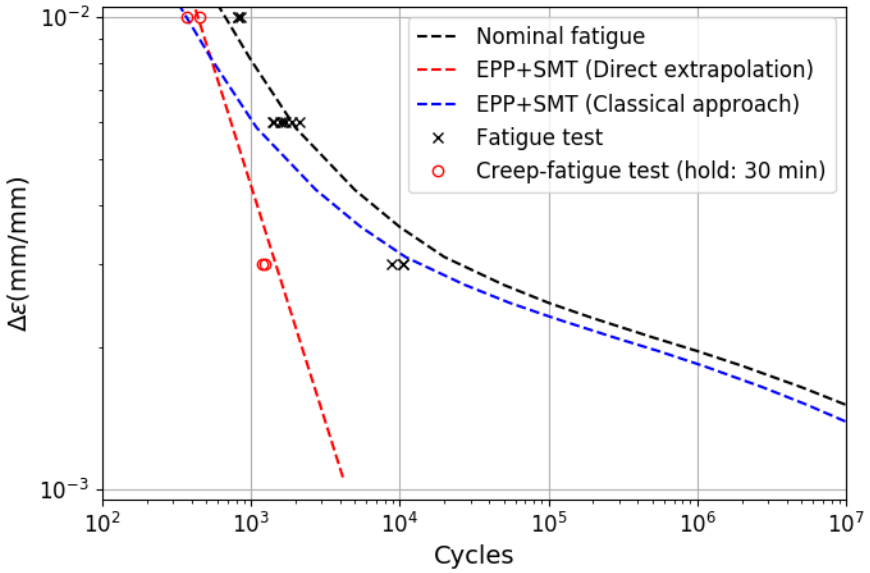

Figure 2.11: Nominal EPP-SMT curves compared with creep-fatigue (i.e. $q = 1$) experimental data for Alloy 617 at 850°C with 30 min hold.

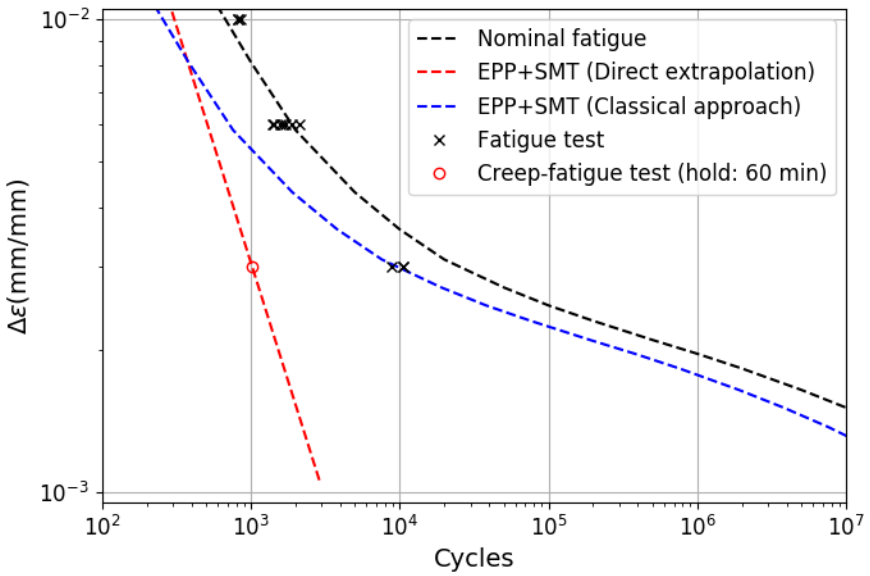

Figure 2.12: Nominal EPP-SMT curves compared with creep-fatigue (i.e. $q = 1$) experimental data for Alloy 617 at 850°C with 60 min hold.

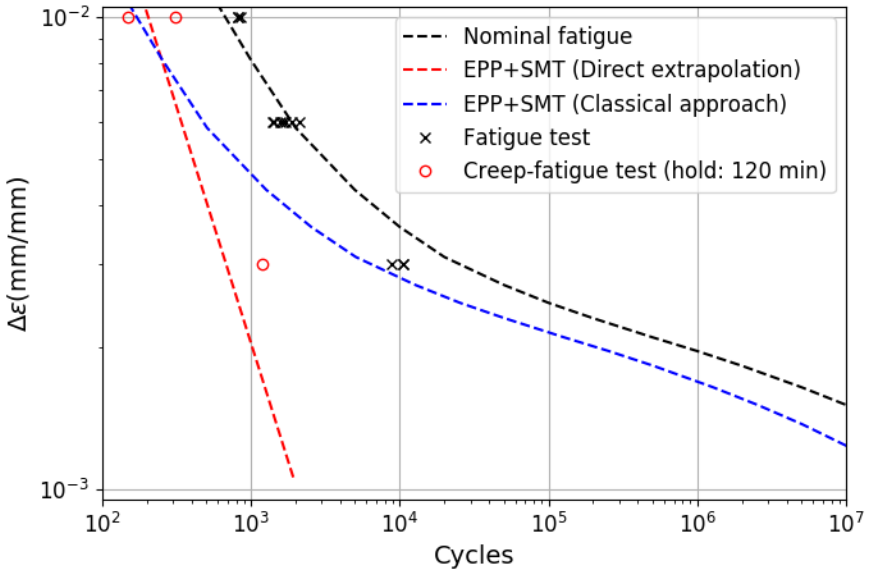

Figure 2.13: Nominal EPP-SMT curves compared with creep-fatigue (i.e. $q = 1$) experimental data for Alloy 617 at 850°C with 120 min hold.

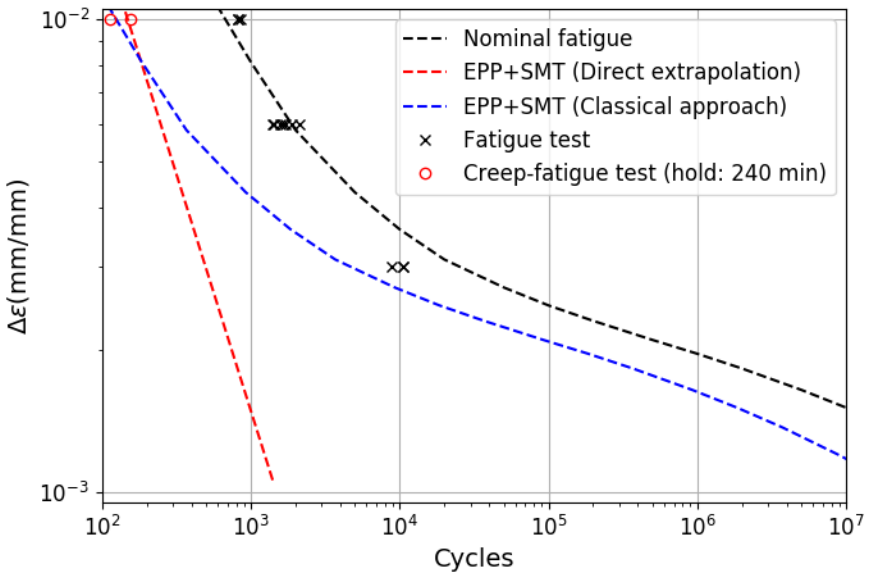

Figure 2.14: Nominal EPP-SMT curves compared with creep-fatigue (i.e. $q = 1$) experimental data for Alloy 617 at 850°C with 240 min hold.

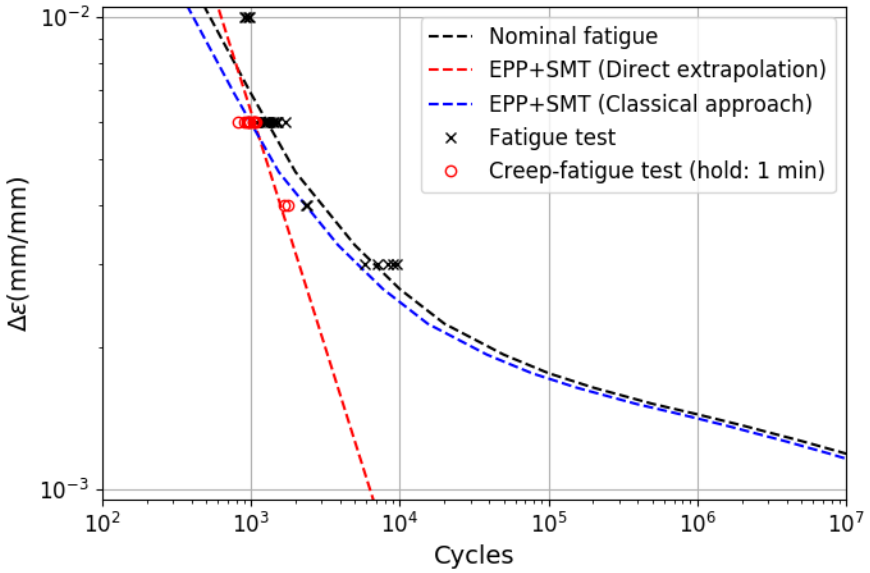

Figure 2.15: Nominal EPP-SMT curves compared with creep-fatigue (i.e. $q = 1$) experimental data for Alloy 617 at 950°C with 1 min hold.

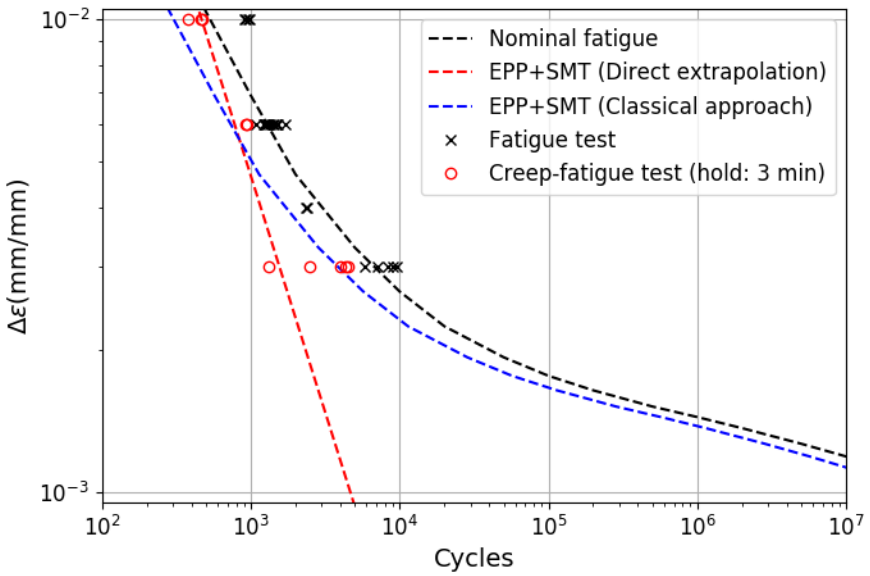

Figure 2.16: Nominal EPP-SMT curves compared with creep-fatigue (i.e. $q = 1$) experimental data for Alloy 617 at 950°C with 3 min hold.

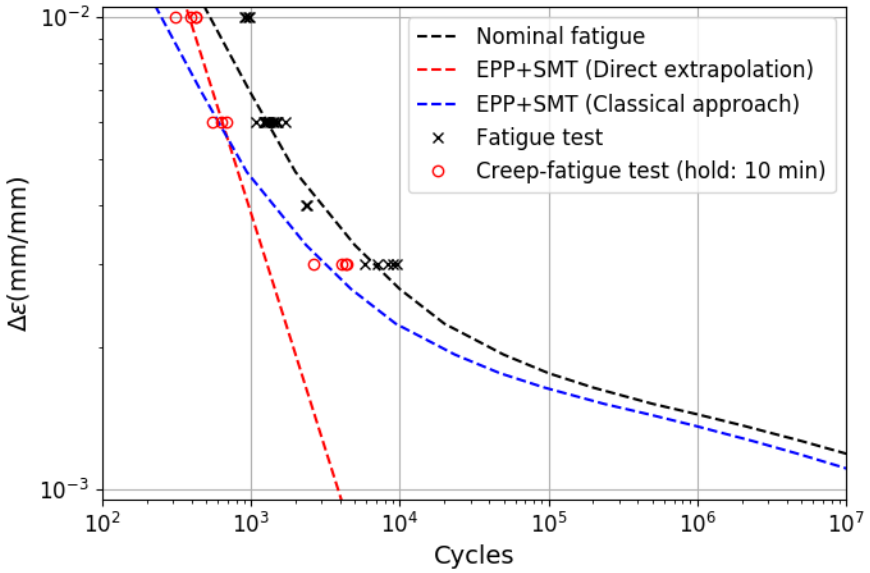

Figure 2.17: Nominal EPP-SMT curves compared with creep-fatigue (i.e. $q = 1$) experimental data for Alloy 617 at 950°C with 10 min hold.

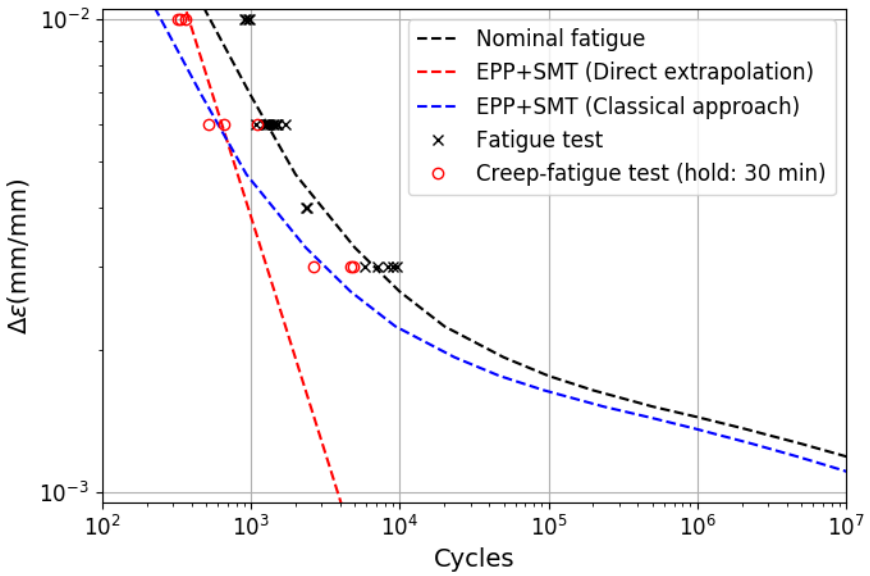

Figure 2.18: Nominal EPP-SMT curves compared with creep-fatigue (i.e. $q = 1$) experimental data for Alloy 617 at 950°C with 30 min hold.

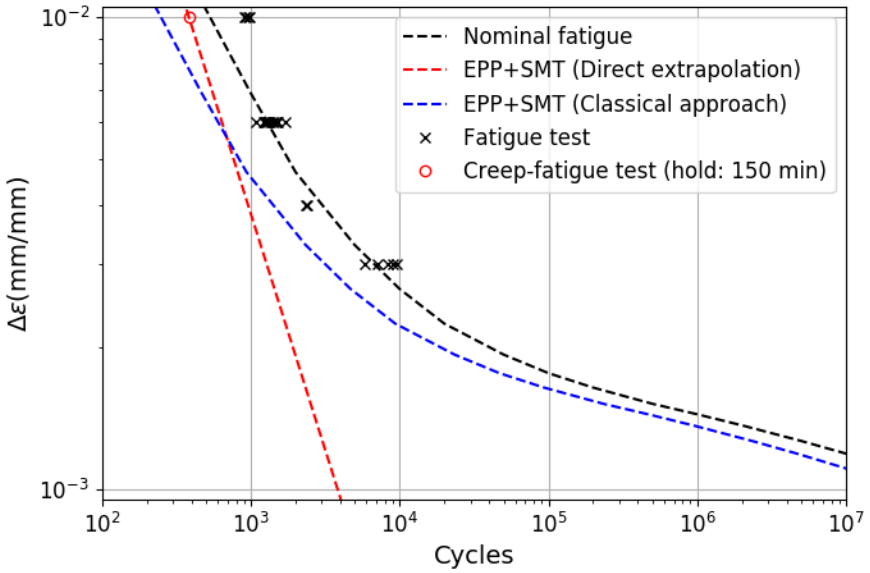

Figure 2.19: Nominal EPP-SMT curves compared with creep-fatigue (i.e. $q = 1$) experimental data for Alloy 617 at 950°C with 150 min hold.

2.3.2 Comparison with SMT tests

Figure 2.20 to Figure 2.27 plot nominal EPP-SMT curves extrapolated for different hold times and follow ups using both direct extrapolation and classical approaches. The figures compare the EPP-SMT curves with the test data. Similar to the comparisons for the creep-fatigue test data, as discussed in Section 2.3.2, both extrapolation approaches predict a cyclic life reasonably close to the experimental data for strain range equal to 0.2% or higher, given the general uncertainty in SMT test data. This validates the use of simple $\frac{1}{q}$ rule – as in Equations 2.5 and 2.6 for the direct extrapolation and classical approaches, respectively – to predict the effect of elastic follow up on the cyclic life. Note $q = 1$ for creep-fatigue tests and $q > 1$ for SMT tests.

Figure 2.23 compares the predicted nominal EPP-SMT curves with the sole experimental data ($\Delta\varepsilon = 0.063\%$) available in the very low strain range regime. As indicated by the figure, the classical approach over predicts the cyclic life by several orders of magnitude. In contrast, the direct extrapolation approach under predicts the test results although the difference between the predicted and experimental cyclic life is much less compared to that for the classical approach.

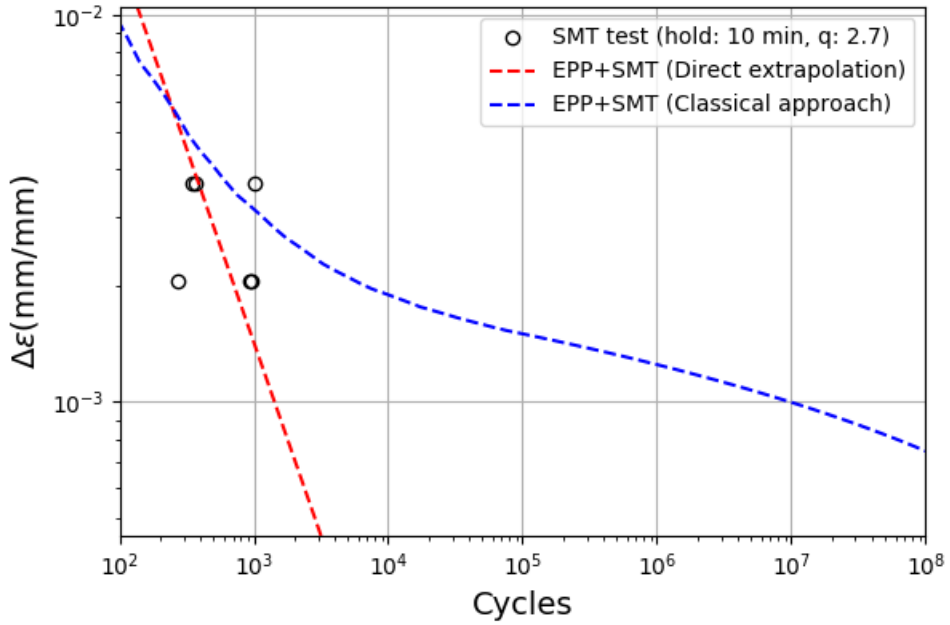

Figure 2.20: Nominal EPP-SMT curves compared with SMT experimental data for Alloy 617 at 950°C with 10 min hold and follow up factor of 2.7.

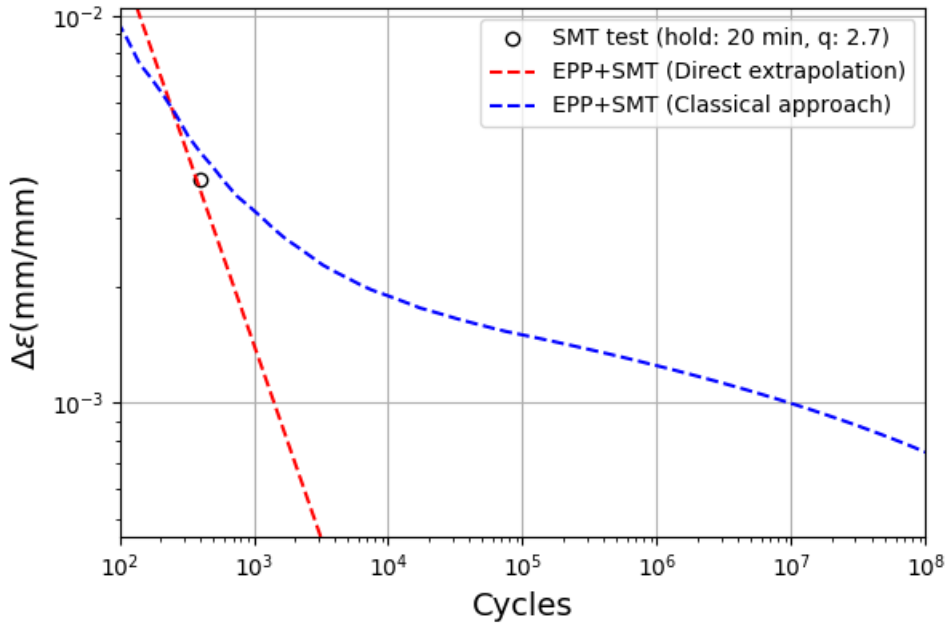

Figure 2.21: Nominal EPP-SMT curves compared with SMT experimental data for Alloy 617 at 950°C with 20 min hold and follow up factor of 2.7.

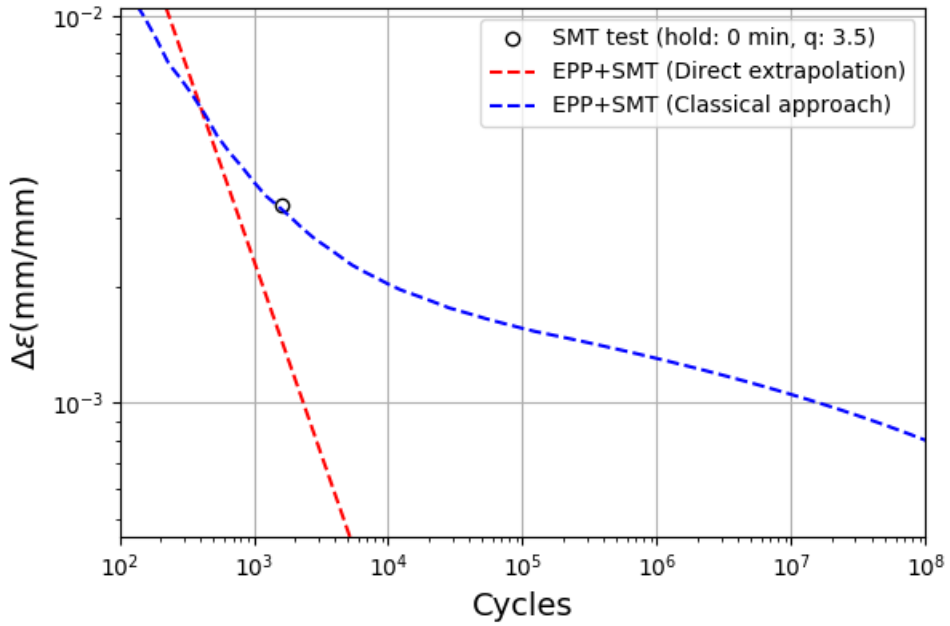

Figure 2.22: Nominal EPP-SMT curves compared with SMT experimental data for Alloy 617 at 950°C with 0 min hold and follow up factor of 3.5.

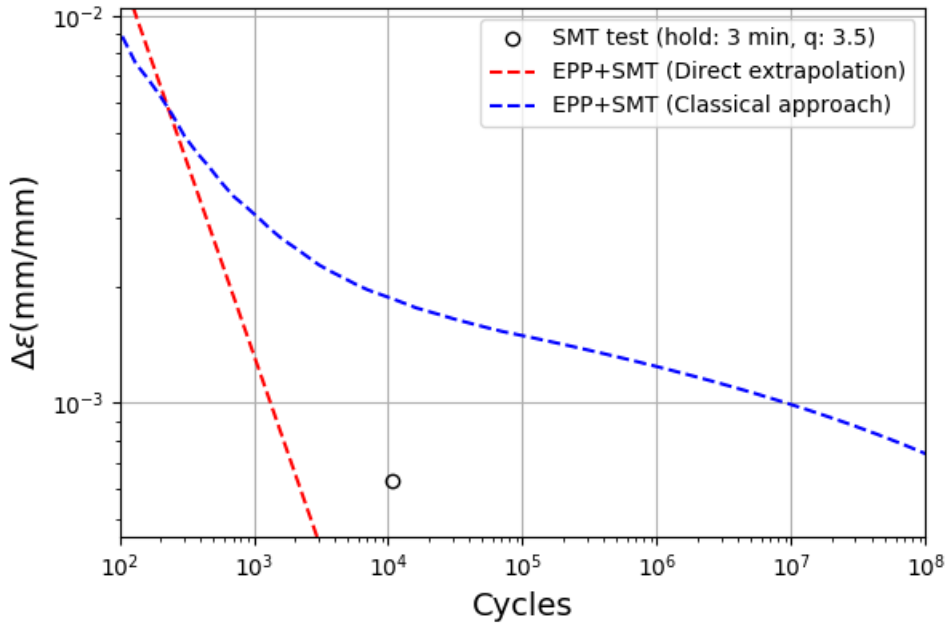

Figure 2.23: Nominal EPP-SMT curves compared with SMT experimental data for Alloy 617 at 950°C with 3 min hold and follow up factor of 3.5.

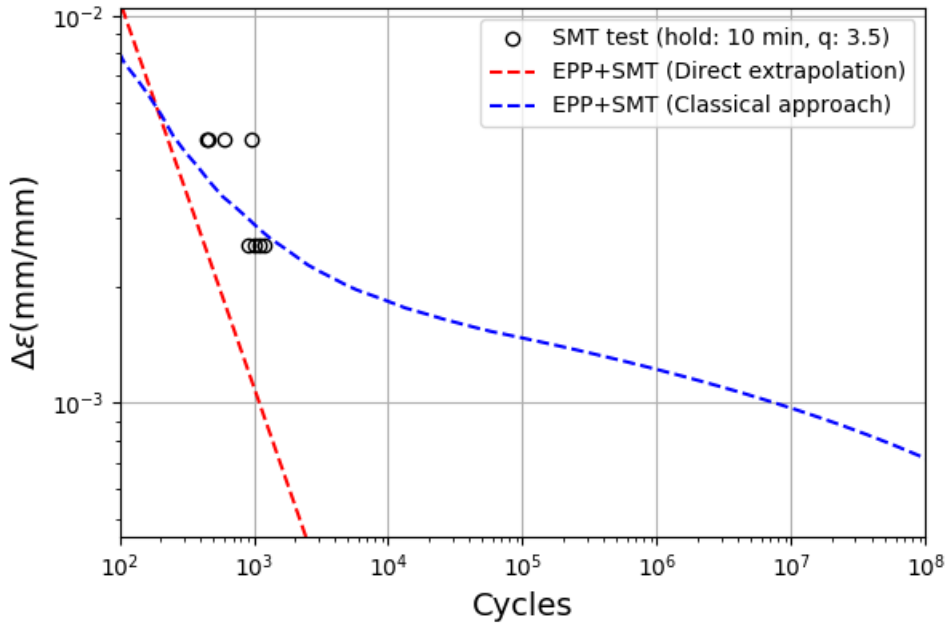

Figure 2.24: Nominal EPP-SMT curves compared with SMT experimental data for Alloy 617 at 950°C with 10 min hold and follow up factor of 3.5.

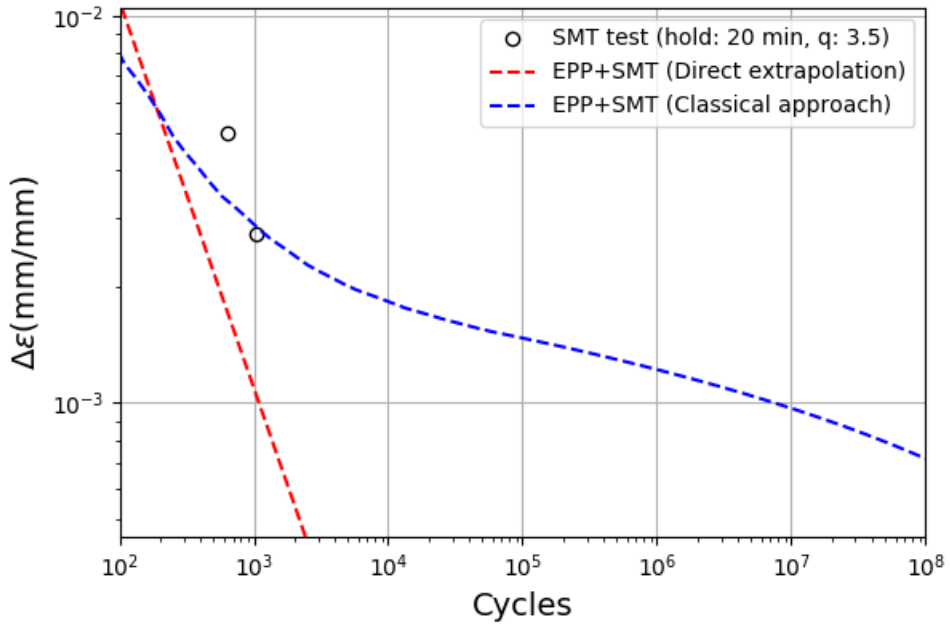

Figure 2.25: Nominal EPP-SMT curves compared with SMT experimental data for Alloy 617 at 950°C with 20 min hold and follow up factor of 3.5.

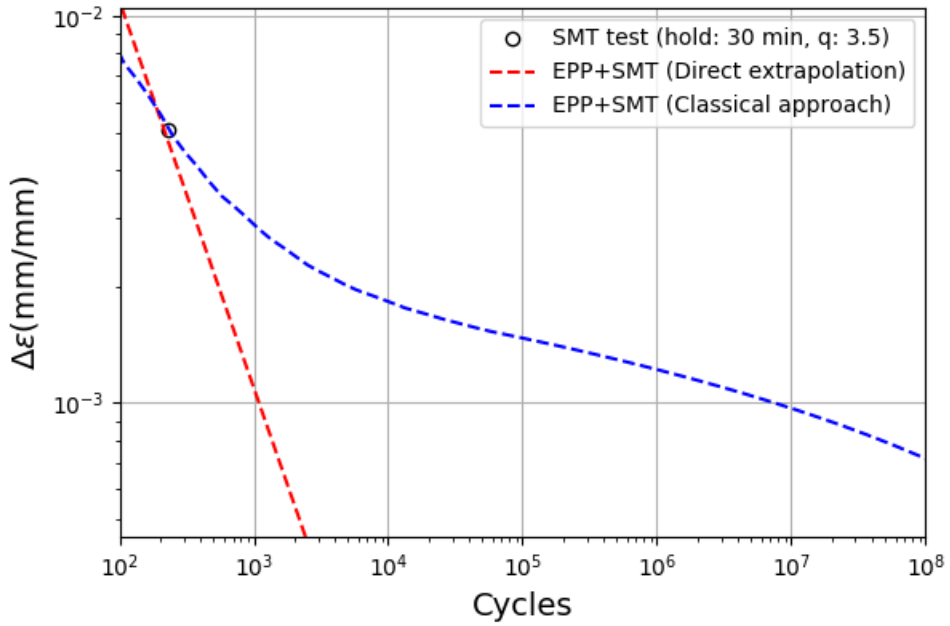

Figure 2.26: Nominal EPP-SMT curves compared with SMT experimental data for Alloy 617 at 950°C with 30 min hold and follow up factor of 3.5.

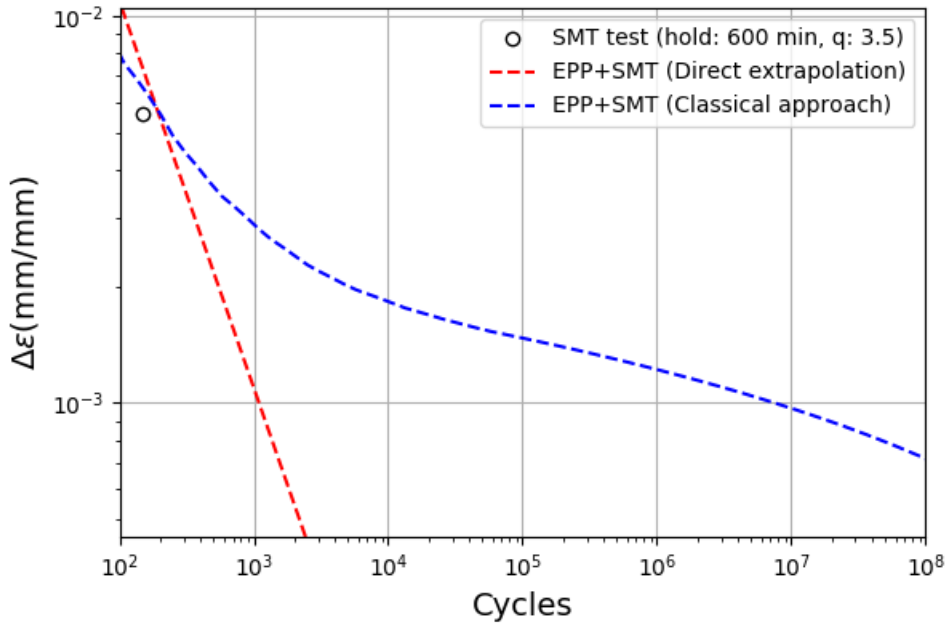

Figure 2.27: Nominal EPP-SMT curves compared with SMT experimental data for Alloy 617 at 950°C with 600 min hold and follow up factor of 3.5.

2.3.3 Preliminary design curves

The discussion above indicates both the extrapolation approaches reasonably capture the experimental results in the high strain range regime. In the low strain range regime, a conclusion could not be reached mostly due to the lack of data. At the same time generating considerable amount of data in the low strain range regime is practically impossible due to long test duration. Therefore, an engineering judgement should be called which should provide a conservative, but not overly-conservative, estimate of the cyclic life, specifically when compared to current design methods. Based on the nominal EPP-SMT curves plotted in Figure 2.5 to Figure 2.27 a conservative approach would be to use the lesser of the cycles to failure predicted by two approaches, which means use the classical approach for very high range and use the direct extrapolation approach for the rest. This is reasonable considering the lack of data in the low strain range regime, the direct extrapolation approach bounding almost all the test data, and the only available data in the low strain range regime (see Figure 2.23) being comparatively close to the nominal EPP-SMT curve constructed using the direct extrapolation approach.

The nominal EPP-SMT curves are based on average properties and therefore a design margin must be applied to the nominal curves for constructing the EPP-SMT design charts for creep-fatigue design evaluation. The ASME Code applies a factor of 2 on strain range and 20 on cycles for constructing the fatigue design curves which are used to calculate the fatigue damage fraction using the strain range determined in the component analysis. The Code also increases the stress relaxation history by a factor of 0.9 for design by elastic analysis and design by EPP analysis, and a factor of 0.67 for design by inelastic analysis for calculating creep damage fraction using 95% confidence prediction lower bound rupture properties. The creep and fatigue damage fractions are then compared with the creep-fatigue damage envelope in the creep-fatigue interaction diagram

(also called "D" diagram) for the design check. No design margin is applied to the "D" diagram, essentially directly constructed from creep-fatigue test data base. For the EPP-SMT design method we propose to retain the design margin applied to the average fatigue curves and apply no additional margin for creep damage. Although future work will determine if an additional design factor is required for the EPP-SMT method to cover the additional margin the ASME Code applies on the creep damage, the proposed approach of using the minimum of the cyclic lives predicted by the two extrapolation approaches may well cover this additional design margin. This is verified in Chapter 3 via a comparative study of the design methods for two sample problems.

Figure 2.28 to Figure 2.30 plot the preliminary EPP-SMT design curves for Alloy 617 at 800°C, 850°C, and 950°C, respectively. The preliminary design curves are plotted for different follow up factors and hold times using:

$$N_{SMT,design} = \min\left\{N_{SMT,design}^{Direct},\ N_{SMT,design}^{Classical}\right\} \tag{2.8}$$

$N_{SMT,design}^{Direct}$ in Equation 2.8 is the cycles to failure determined using the direct extrapolation approach and after applying the design margins:

$$N_{SMT,design}^{Direct} = \left\{\frac{1}{20} * N_{SMT,nominal}^{Direct}(\Delta\varepsilon),\ N_{SMT,nominal}^{Direct}(2 * \Delta\varepsilon)\right\} \tag{2.9}$$

which can be deduced to:

$$N_{SMT,design}^{Direct} = \frac{1}{20}\frac{1}{q}\frac{C}{\Delta\varepsilon}\frac{(\frac{1}{1+t_h})^p + D}{1+D} \tag{2.10}$$

using Equation 2.5. $N_{SMT,design}^{Classical}$ in Equation 2.8 is the cycles to failure using the classical approach which shifts the design fatigue curve using:

$$N_{SMT,nominal}^{Classical} = N_{fatigue,design}\left\{\frac{1}{q}\frac{(\frac{1}{1+t_h})^p + D}{1+D}\right\} \tag{2.11}$$

Note additional test data in the low strain range regime are required for verifying and improving the extrapolation procedure used for these preliminary design curves. The hold time for these low strain range tests can be selected based on the stress relaxation profile, determined from the Code isochronous stress-strain relationship, under the same strain range to be used in creep-fatigue or SMT tests. Since the accumulation of creep damage reduces with stress relaxation, at some relaxed stress the damage accumulation becomes negligible. This information can be used to carefully choose the hold time that is sufficiently long enough for the stress to relax during the hold but short enough for the test to complete in reasonable time.

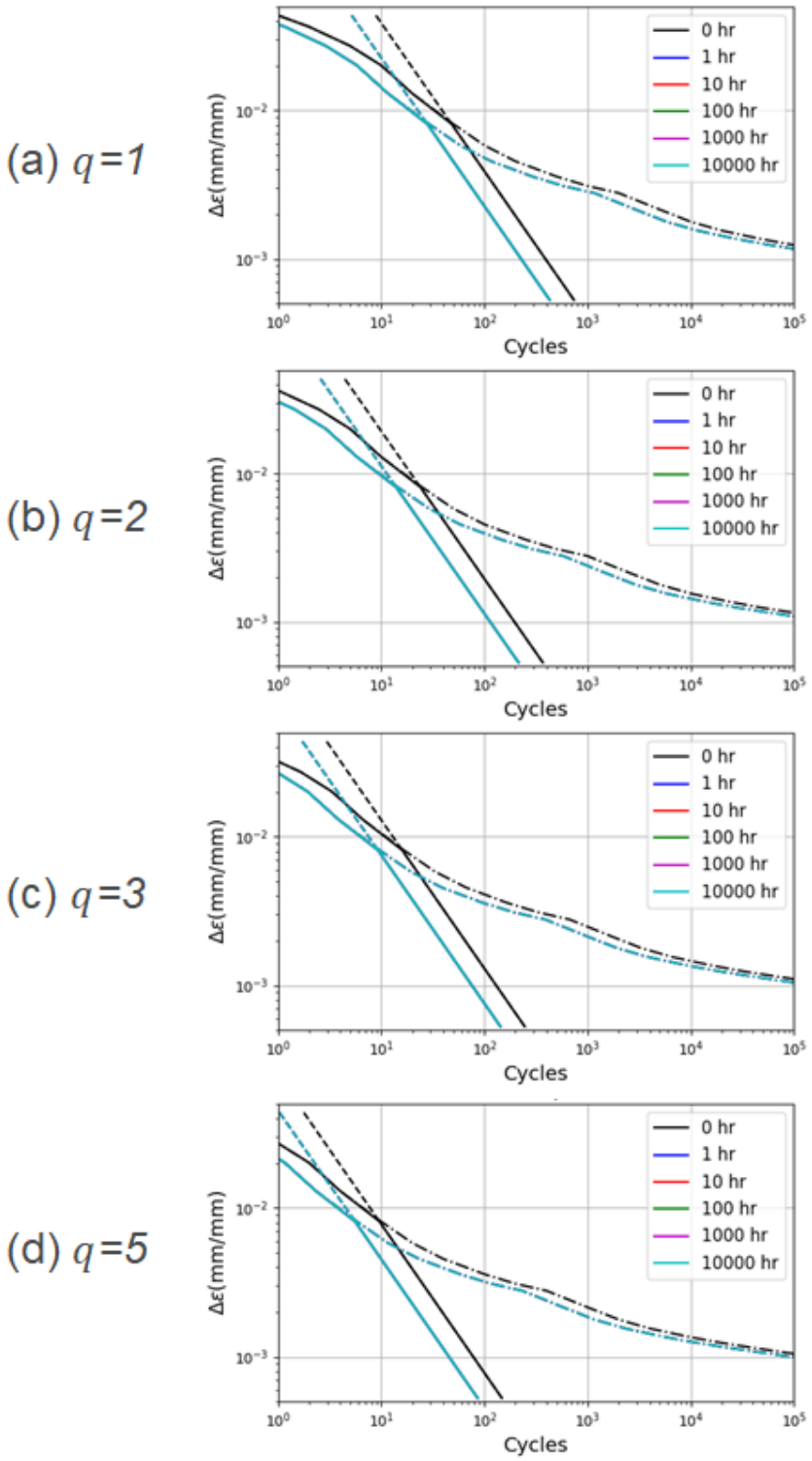

Figure 2.28: Preliminary EPP-SMT design curves (solid lines) at 800°C for different hold times and elastic follow ups. Dashed and dash-dotted lines represent curves constructed using direct extrapolation and classical approach, respectively.

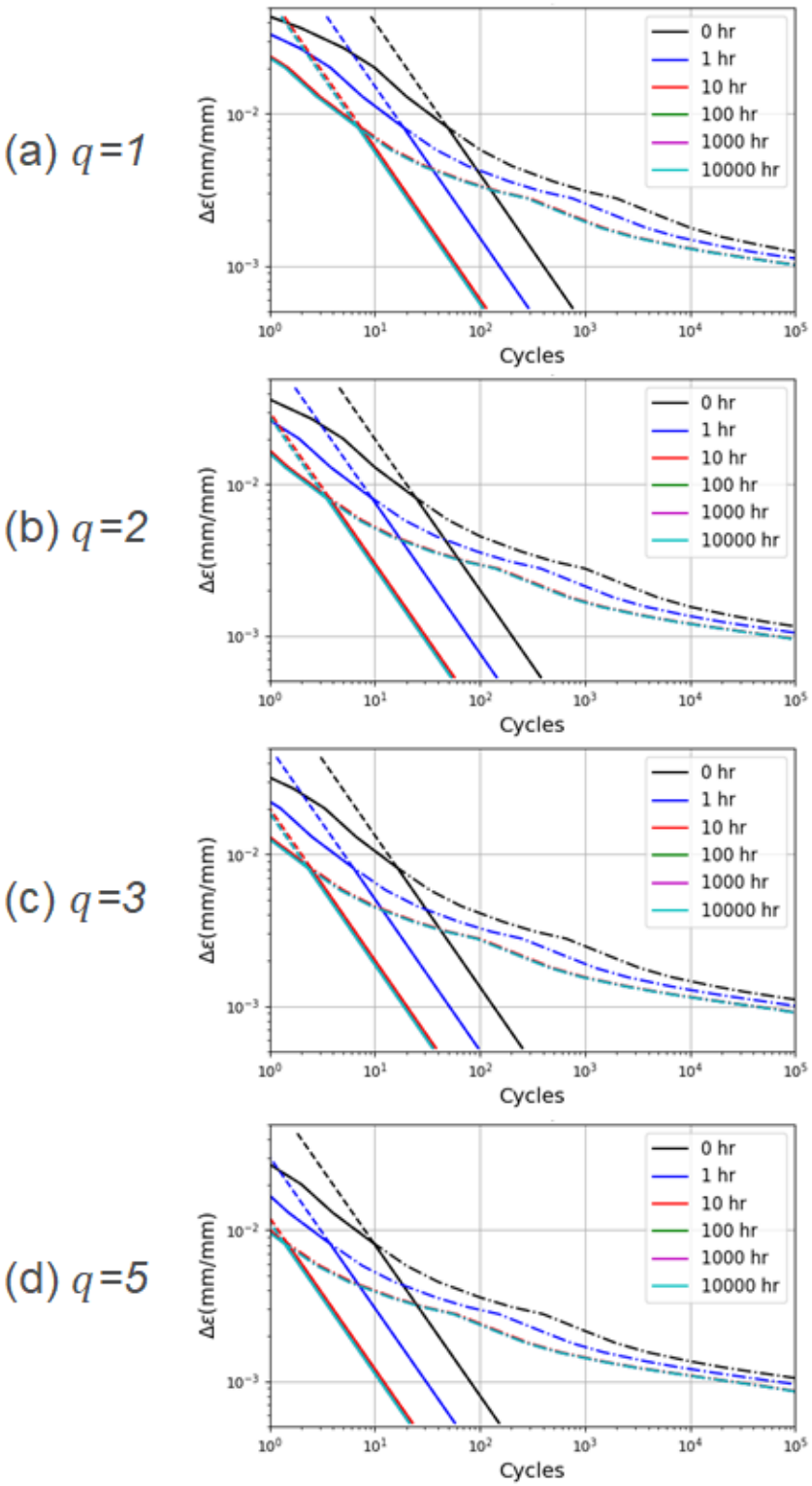

Figure 2.29: Preliminary EPP-SMT design curves (solid lines) at 850°C for different hold times and elastic follow ups. Dashed and dash-dotted lines represent curves constructed using direct extrapolation and classical approach, respectively.

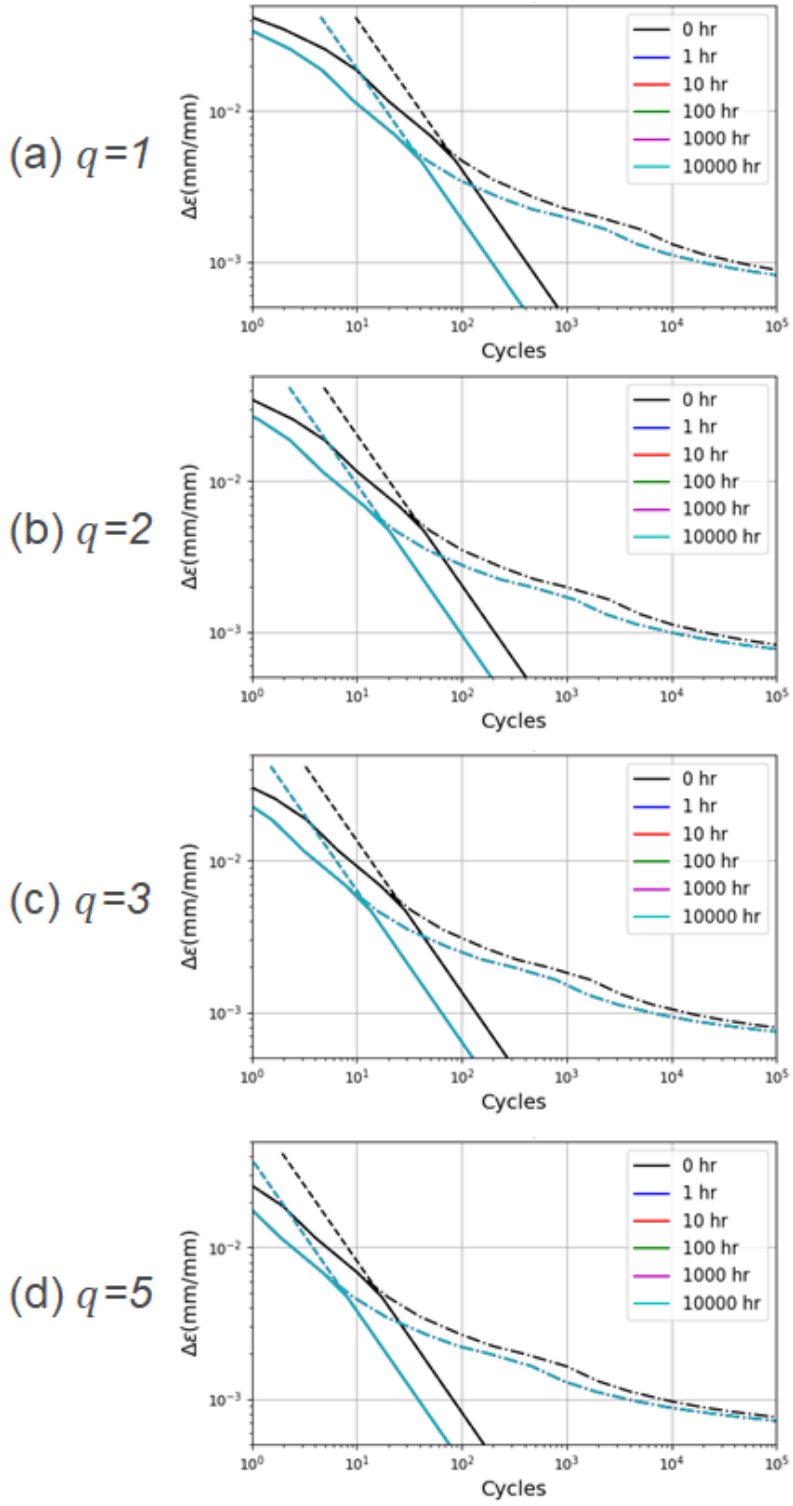

Figure 2.30: Preliminary EPP-SMT design curves (solid lines) at 950°C for different hold times and elastic follow ups. Dashed and dash-dotted lines represent curves constructed using direct extrapolation and classical approach, respectively.

A comparison among the preliminary design curves, plotted in Figure 2.28 to Figure 2.30, for different temperatures indicates the estimated life would be shorter at 850°C than that at 950°C for all the hold times except for the fatigue design curve (i.e. hold time = 0 hour). However, one would expect shorter cyclic life at higher temperature. To further investigate this, the creep-fatigue test data at different temperatures with same hold times are plotted in Figure 2.31 to Figure 2.32. Due to lack of data comparisons were not made for other hold times. The figures indicate shorter cyclic life at 850°C than 950°C for 0.3% strain range although at 1% strain range the cyclic life is about the same for both temperatures. This means larger shifts for the EPP-SMT curves at 850°C to account for the creep damage during the hold and therefore shorter estimated cyclic life compared to that at 950°C. However, confirming this counter intuitive trend requires further investigation such as comparing the stress relaxation profiles and respective creep damage fraction based on average rupture properties between the two temperatures.

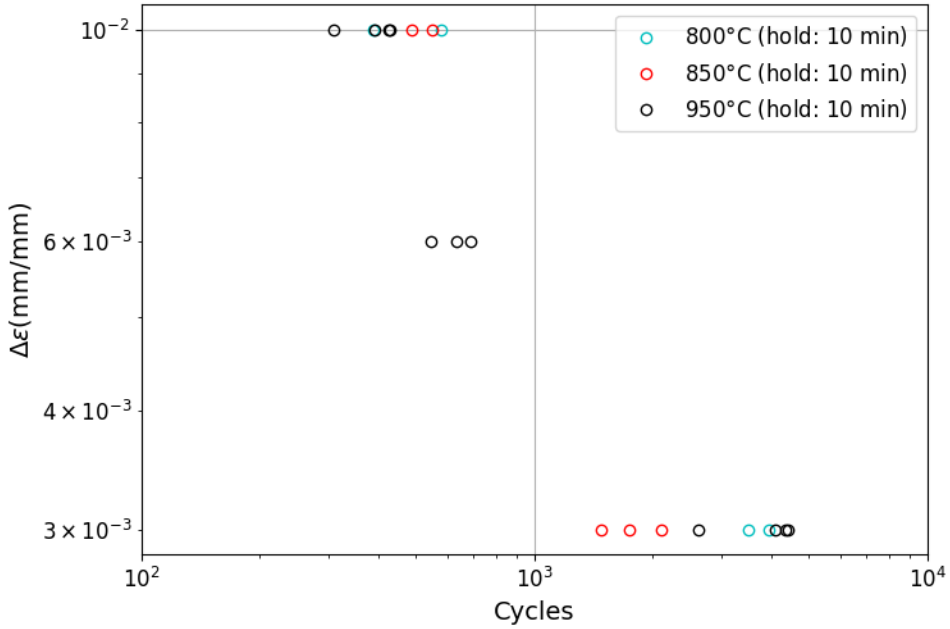

Figure 2.31: Alloy 617 creep-fatigue test data at different temperatures for a hold time equal to 10 minutes.

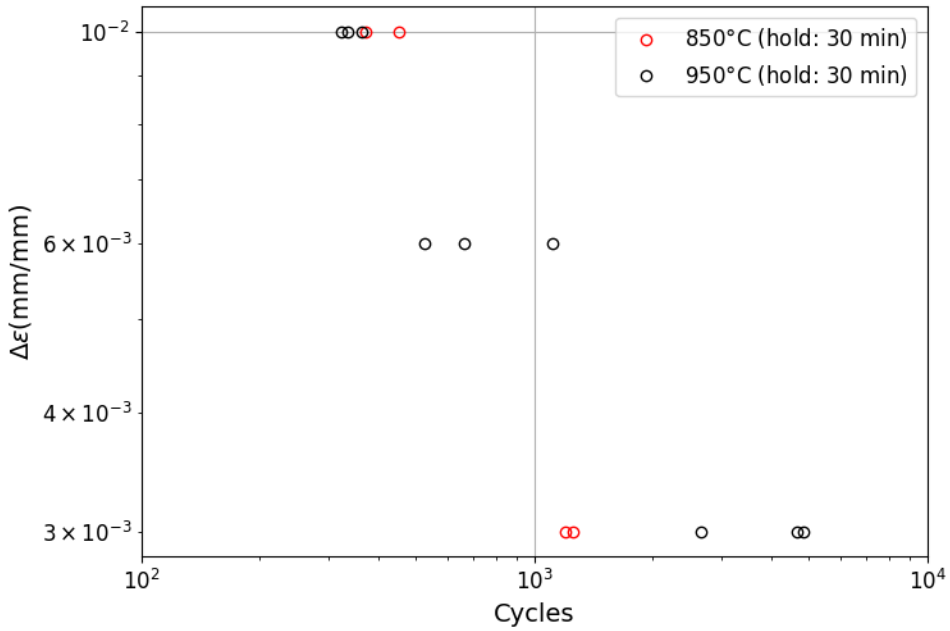

Figure 2.32: Alloy 617 creep-fatigue test data at different temperatures for a hold time equal to 30 minutes.

3 Comparison with ASME methods through component analysis

Since creep-fatigue and SMT tests with long holds in the low strain range regime are not practically possible due to the very long test duration, an indirect way of validating the preliminary EPP-SMT design charts would be performing comparative design analysis for structural components under loading conditions as typical for nuclear reactor structural components. This chapter presents results from such comparative analysis for a simple structure – a long cylinder – as well as for a complex structure – a flat head vessel. Two sets of comparisons were made for the creep-fatigue life estimation of the structures – best estimate life and design life. For the best estimate life calculations average material properties were used, while design life calculations are based on properties factored with design margin. Creep-fatigue life using EPP-SMT approach was calculated for both extrapolation approaches discussed above to determine which approach estimates life comparable to other methods.

3.1 Creep-fatigue life estimation methods

Section III, Division 5 [1] and associated nuclear Code cases [2] describe three methods for creep-fatigue design checks – design by elastic analysis, design by elastic perfectly-plastic (EPP) analysis, and design by inelastic analysis – for components in high temperature nuclear service. We selected the design by elastic analysis and design by inelastic analysis to compare with EPP-SMT design method. For best estimate life calculations, we modeled the material with the same inelastic model used in design by inelastic analysis. The best estimate life from inelastic analysis was compared with life estimated following the analysis method used in EPP-SMT design but using nominal EPP-SMT curves instead of design curves. The life estimation process for each method is briefly discussed below.

3.1.1 Design by elastic analysis

The design by elastic analysis method is provided in Section III, Division 5, Subsection HB, Subpart B Nonmandatory Appendix-T of ASME Code [1]. This method uses creep-fatigue interaction diagram for creep-fatigue design check. The total accumulated creep damage, D_c and fatigue damage, D_f must satisfy:

$$D_c + D_f \leq D \tag{3.1}$$

where D is the total creep-fatigue damage bounded by the damage envelop in the creep-fatigue interaction diagram. For Alloy 617 the Code uses a bilinear interaction diagram, as illustrated by Figure 3.1, with an intersection point of (0.1, 0.1). The creep-fatigue damage envelop is determined from creep-fatigue test data without applying any margin but with bounding all the test results.

The design process starts with performing an elastic stress analysis of the component for each service load types. The resulting equivalent strain range computed using the equation provided in HBB-T-1413 is then adjusted to account for the creep and plasticity. The modified strain range is

used to determine design allowable number of cycles from design fatigue curve. The total fatigue damage fraction, D_f is then computed using Miner rule:

$$D_f = \sum_{j=1}^{p} \left(\frac{n}{N_d}\right)_j \tag{3.2}$$

where $(n)_j$ is the number of repetitions and $(N_d)_j$ is the number of design allowable cycles for cycle type j.

To calculate creep damage, the Code uses the same modified strain range to determine a stress relaxation profile from the isochronous stress-strain curves, or from a relaxation analysis, or from a global relaxation analysis, if it meets the conditions. Then, allowable time durations at various stress level in the stress relaxation profile are determined from rupture stress-time design charts. Using the allowable time durations, creep damage is calculated according to life-fraction rule:

$$D_c = \sum_{k=1}^{q} \left(\frac{\Delta t}{T_d}\right)_k \tag{3.3}$$

where $(\Delta t)_k$ is the time duration and $(T_d)_k$ is the allowable time duration for the stress occurring at time interval, k. The rupture stress-time design charts are based Larson-Miller fit to the creep rupture test data and taking the 95% confidence prediction lower bound values. To apply design margin on the creep damage the Code, therefore, increases the stress relaxation profile by a factor of $\frac{1}{0.9}$. Once both fatigue and creep damages are computed, the creep-fatigue interaction diagram is used to determine whether the design passes the creep-fatigue damage check.

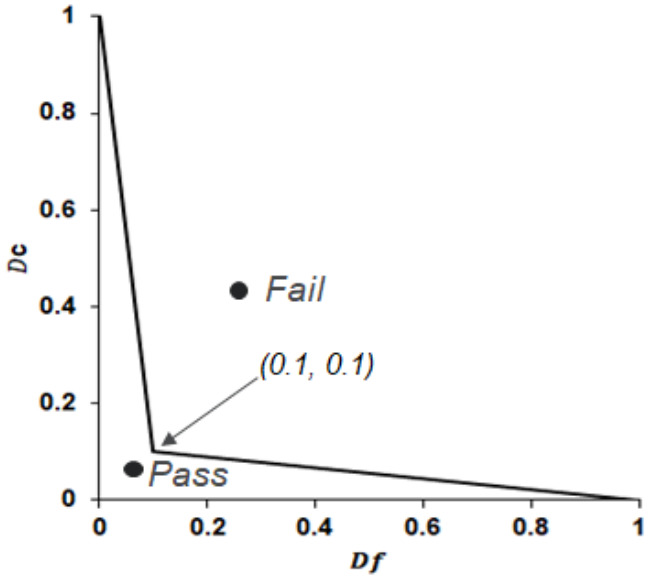

Figure 3.1: Alloy 617 creep-fatigue interaction diagram used in current creep-fatigue design methods.

The thermal and structural properties of Alloy 617 for performing elastic analysis are taken from Alloy 617 Code Case [15]. The design fatigue charts to calculate fatigue damage fraction and the rupture stress-time chart to compute creep damage fraction are also from Alloy 617 Code case.

3.1.2 Design by inelastic analysis

Section III, Division 5, Subsection HB, Subpart B Nonmandatory Appendix-T of ASME Code [1] also contains the rules for design by inelastic analysis. This method uses the same creep-fatigue interaction diagram, as shown in Figure 3.1 and expressed by Equation 3.1, used in design by elastic analysis method. It also calculates fatigue damage using Miner's rule (Equation 3.2) and creep damage using time fraction rule (Equation 3.3). However, the material model to be used in the analysis is different. An inelastic constitutive model capable of capturing the material response under high temperature cyclic load should be used in the analysis. Moreover, instead of simulating individual service load cases as in design by elastic analysis method, the design of inelastic method requires simulating the full service load history of the component or until a steady cyclic response is achieved in the case of repeating service load.

The simulated stress and strain histories are used to calculate the creep and fatigue damage fractions. The Code uses a rainflow counting and Miner's rule to determine the fatigue damage fraction from the equivalent strain range, computed from the simulated strain history, and using the design fatigue curves. For creep damage calculation the Code uses Huddleston's approach to convert the stress tensor into a scalar measure to account for the effect of triaxiality on creep rupture life. Then, the scalar stress relaxation profile is converted into creep damage using the Code life-fraction rule and rupture stress-time design chart. Design by inelastic method applies a larger margin on the stress relaxation history – stress is divided by 0.67 instead of 0.9 used in design by elastic analysis.

As discussed above, the inelastic analysis requires an inelastic constitutive model. Assembling a complete inelastic model capable of accurately capturing details of elevated temperature cyclic plasticity and creep is a very complicated task. We, therefore, used a simplified description of the material response which takes advantage of the steady cyclic response of the system. The simplified inelastic model of Alloy 617, developed at ANL, is based on an additive, history-independent decomposition of the total strain, ε into elastic, time-independent plastic, and time-dependent creep parts:

$$\varepsilon = \varepsilon_e + \varepsilon_p + \varepsilon_c \tag{3.4}$$

where the elastic strain, ε_e is determined using Young's modulus and Poisson's ratio; the time-independent plastic strain, ε_p is based on simple J_2 plasticity with a Voce hardening model:

$$\sigma_{flow} = \sigma_o + R(1 - e^{-\delta \varepsilon_p}) \tag{3.5}$$

where σ_{flow} is the flow stress and σ_o, R, and δ are constants; and the time-dependent creep strain, ε_c is based on a creep model adopted from a form developed by Kocks [21] and Mecking [22]:

$$\dot{\varepsilon_c} = \dot{\varepsilon_o} e^{\frac{B\mu b^3}{AkT}} \left(\frac{\sigma}{\mu}\right)^{\frac{-\mu b^3}{AkT}} \tag{3.6}$$

where μ is the material shear stress, k is the Boltzmann constant, T the absolute temperature, b is a characteristic Burgers vector, and $\dot{\varepsilon}_0$ is some reference strain rate. Table 3.1 and Table 3.2 list the parameters for the inelastic model.

T (°C)	σ_o (MPa)	R (MPa)	δ
850	137.393	2.194	1057.483
900	96.749	0.614	3684.582
950	66.862	0.282	7374.702

Table 3.1: Voce model parameters used for Alloy 617 simple inelastic model.

Parameter	Value
$\dot{\varepsilon}_0$	$3.60\text{x}10^{8}$ hrs^{-1}
A	-10.771
B	-1.205
b	$2.470\text{x}10^{-7}$ mm
k	$1.3806\text{x}10^{-20}$ mJ/K

Table 3.2: Creep model parameters used for Alloy 617 simple inelastic model.

3.1.3 EPP-SMT design

Chapter 5 provides the step-by-step procedures for EPP-SMT design method. This prospective design method combines the EPP methodology with the SMT test methodology to avoid the use of D-diagram for creep-fatigue evaluation which requires separate evaluation of creep and fatigue damage and also is over conservative. The method uses EPP-SMT design charts, constructed from creep-fatigue and SMT test data, for creep-fatigue damage evaluation using the equivalent strain range computed through EPP analysis. The EPP analysis is used to bound the structural response for plasticity and creep using a pseudoyield stress, determined from isochronous stress-strain curve according to the procedure described in Chapter 5. The method uses a usage fraction rule for creep-fatigue design check:

$$D = \sum_{j=1}^{n_j} \sum_{i=1}^{n_i} \frac{w_i^j}{N_i^j} \tag{3.7}$$

where w is the number of repetition and N is the total number of allowable cycles for load type i that is included in defining composite cycle type j. N is determined by entering the EPP-SMT design chart for the maximum metal temperature occurring over j and the hold time equal to the cycle period at the equivalent strain range determined following the procedure described in Chapter 5. The design passes if total damage, D is less than or equal to 1.

Note, we considered a single load cycle for the comparative design study presented in this chapter. Therefore, Equation 3.7 simplifies to $D = \frac{w}{N}$. We computed two sets of design lives – one using the EPP-SMT design curves constructed via the direct extrapolation approach and another using the EPP-SMT design curves constructed via classical approach. The design curves are provided in Figure 2.28 to Figure 2.30.

3.1.4 Best estimate life

Best estimate life is essentially the life estimated using average material properties and no explicit design margin. We computed best estimate life from inelastic analysis using the inelastic model described above and following the creep-fatigue damage evaluation of design by inelastic analysis, but without applying any design margin.

We also estimated the creep rupture life with the EPP-SMT design method but used EPP-SMT nominal curves instead of design curves, as this estimated life is compared with the best estimate life from inelastic analysis.

3.2 Component geometries and loading conditions

We performed the comparative study of design methods on two different structures under different thermal and pressure loading conditions. The first structure is a long cylinder with 50 mm thickness and 1000 mm diameter. This simple structure does not have any localized stress concentration and therefore the comparative study on this structure will help examine the extrapolation procedures for EPP-SMT curves without considering the effect of elastic follow up.

The second structure considered for this comparative study is a flat head vessel. Figure 3.2 shows the geometry of the flat head vessel. The knuckle of the flat head vessel experiences a localized increase in stress due to sudden change in the cross section. Therefore, this is an interesting problem for investigating the follow up factor for EPP-SMT design method.

Figure 3.3 shows the schematic of the cyclic thermal and pressure loadings applied to the structures. We considered a hold time of 1000 hr. We estimated the creep-fatigue life of the structures for different sets of loading conditions – applied by varying the inner pressure and through thickness temperature gradient, as indicated by P and ΔT in Figure 3.3, respectively.

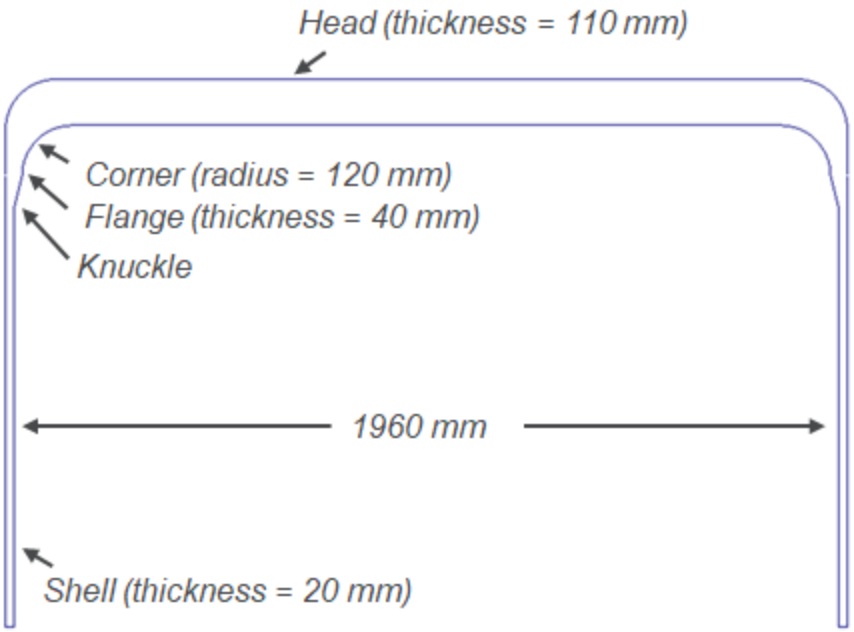

Figure 3.2: Geometry of the flat head vessel.

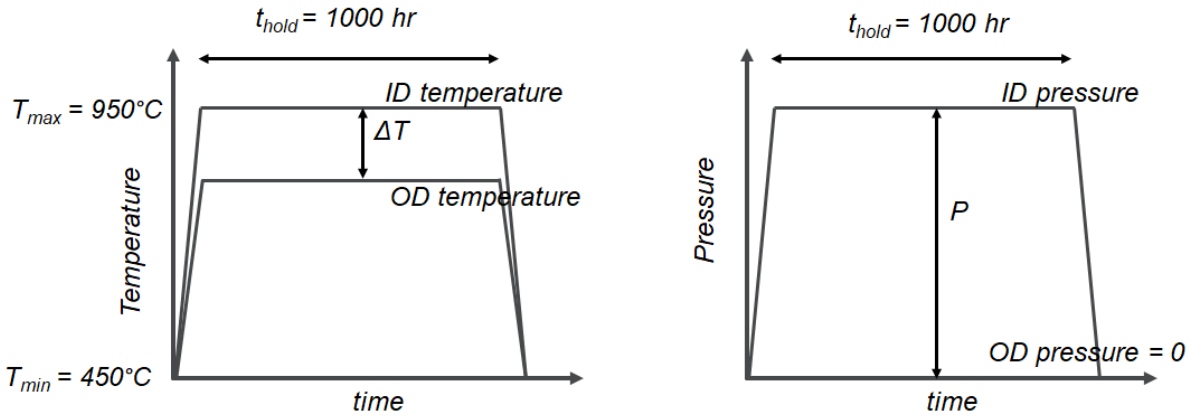

Figure 3.3: Applied thermal and pressure loading profiles.

3.3 Creep-fatigue life comparison

Table 3.3 compares the best-estimate creep-fatigue life of the long cylinder computed from inelastic simulation with the life estimated from EPP-SMT method using the nominal curves. The comparison is made for different loading conditions. Since the cylinder is a very simple structure without any stress concentration, we considered no effect of elastic follow up, i.e. $q = 1$, in the EPP-SMT based life evaluation. The table indicates the extrapolation approach estimates a lower cyclic life than the classical approach for all the loading cases. The steady cyclic strain ranges determined from EPP analysis were found to be very small for all the loading cases,

as indicated by the example results shown in Figure 3.4. These strain ranges fall in the low strain range regime of EPP-SMT curves where the direct extrapolation approach predicts less number of cycles to failure than the classical approach, as discussed in Chapter 2.

Interestingly, creep-fatigue life based on the lesser of the two EPP-SMT approaches is comparable with the best estimate life computed based on inelastic analysis and using the average fatigue and creep rupture properties, as indicated by Table 3.3, for almost all the different loading cases. The loading cases for which the estimated lives are not comparable are marked by asterisk in the table. For these loading cases significant amount of ratcheting was observed in the inelastic simulation, as indicated by the example results shown in Figure 3.5. Since the cycle-to-cycle ratcheting is included in the strain range calculation, the inelastic analysis method predicts much shorter life. This was not the case for EPP-SMT method. However, the two methods should not be compared for these loading cases, as the life of the structure would be controlled by ratcheting limit.

Table 3.4 compares the EPP-SMT design methods with two of the current ASME design methods – design by elastic analysis and design by inelastic analysis – for creep-fatigue evaluation of the long cylinder. The design by elastic analysis method is the most conservative approach among the ASME design methods and hence provides most conservative estimation of the creep-fatigue life. In general, design by inelastic analysis method is less conservative compared to design by elastic analysis method, at least for nuclear service operating condition. However, it still applies a big margin on the stress relaxation profile – dividing the stress by a factor of 0.67 – which may be an overly conservative approach in computing creep-damage from rupture stress-time design chart, particularly with high stress values. However, this was not the case for these sample problems as Alloy 617 relaxes quickly to low stress values at the temperature considered during hold in the loading conditions.

Similar to the best estimate life comparison, the EPP-SMT method with the lesser estimation of the two approaches predicts creep-fatigue life comparable to the inelastic method for all the loading cases except for $P = 0.0\ MPa$, $\Delta T = 25℃$. Note the loading cases marked with asterisk in the table should not be considered for comparison because the design would be controlled by ratcheting check, as discussed above. For $P = 0.0\ MPa$, $\Delta T = 25℃$ loading case the design by inelastic method estimates a design life of 2470 cycles compared to 472 cycles by the EPP-SMT method. This could be due to the over conservatism in the direct extrapolation approach for estimating life in the very low strain range regime. This was also observed for the single experimental data ($\Delta\varepsilon = 0.063\%$) in the very low strain range regime, as indicated by Figure 2.23. The steady cyclic strain range calculated from EPP analysis was about 0.04% for $P = 0.0\ MPa$, $\Delta T = 25℃$ loading condition.

Loading		Best estimate creep-fatigue life (cycles)		
ΔT (°C)	inner P (MPa)	Inelastic analysis (no margin applied on stress relaxation history) + average fatigue and average rupture stress	EPP analysis + nominal EPP-SMT curves based on	
			direct extrapolation	classical approach
			$q = 1$	$q = 1$
100	0	994	812	2.6×10^7
	0.25	1181	800	2.3×10^6
	0.5	1057	784	2.0×10^6
50	0	7728	4017	3.2×10^8
	0.25	4093	3871	2.6×10^8
	0.5*	493	3994	3.1×10^8
25	0	10850	9549	6.4×10^9
	0.25*	3429	9431	6.1×10^9
	0.5*	243	9010	5.1×10^9

Table 3.3: Best estimate creep-fatigue life of the long cylinder compared between inelastic analysis method and EPP-SMT method for different loading conditions. The shaded cells indicate which of the two extrapolation approaches for EPP-SMT curves provides conservative estimation of the creep-fatigue life. The asterisks indicate significant ratcheting observed in inelastic simulation.

Loading		Creep-fatigue design life (cycles)			
ΔT (°C)	inner P (MPa)	ASME design methods		EPP-SMT design method	
		Design by elastic analysis	Design by inelastic analysis	direct extrapolation	classical approach
				$q = 1$	$q = 1$
100	0	0	123	41	5898
	0.25	0	87	40	5084
	0.5	0	24	39	4582
50	0	0	552	201	5.7×10^5
	0.25	0	185	194	3.6×10^5
	0.5*	0	12	200	5.3×10^5
25	0	0	2470	478	1.6×10^8
	0.25*	0	273	472	1.5×10^8
	0.5*	0	6	451	1.0×10^8

Table 3.4: Creep-fatigue design life of the long cylinder compared between current ASME design methods – design by elastic analysis and design by inelastic method – and the prospective EPP-SMT design method for different loading conditions. The shaded cells indicate which of the two extrapolation approaches for EPP-SMT curves provides conservative estimation of the creep-fatigue life. The asterisks indicate significant ratcheting observed in inelastic simulation.

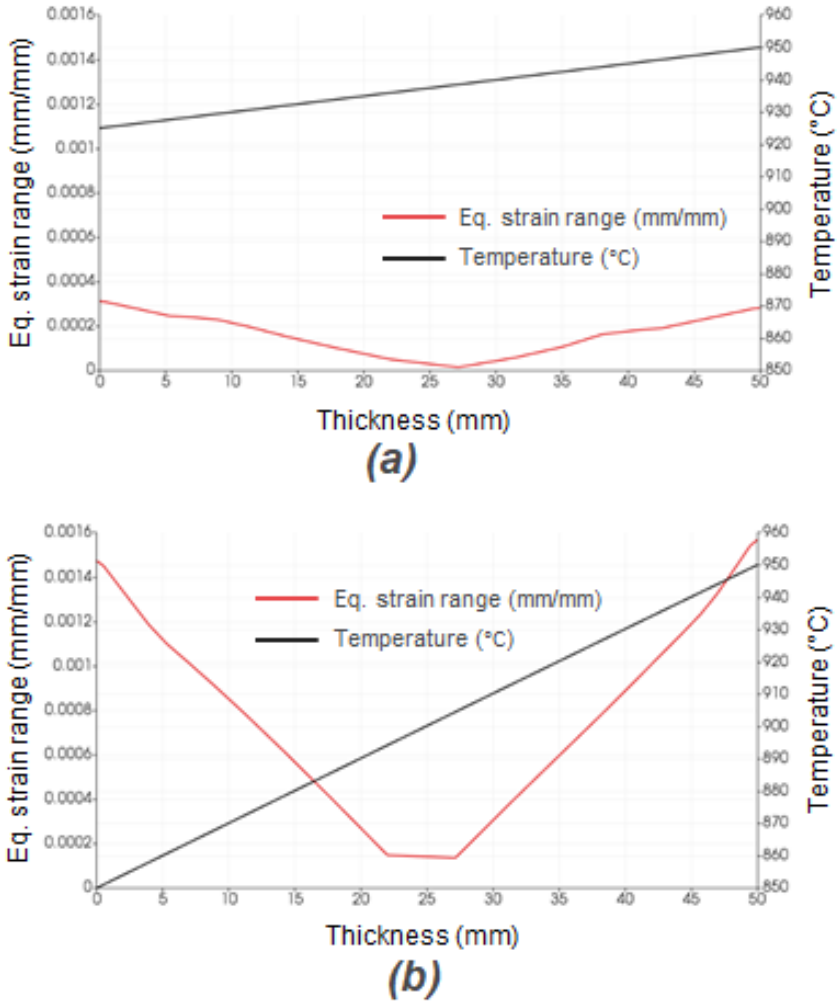

Figure 3.4: Through thickness steady cyclic equivalent strain range computed from EPP analysis of the long cylinder. Loading conditions are (a) $P = 0.0$, $\Delta T = 25℃$ and (b) $P = 0.0$, $\Delta T = 100℃$ following the profiles showed in Figure 3.3.

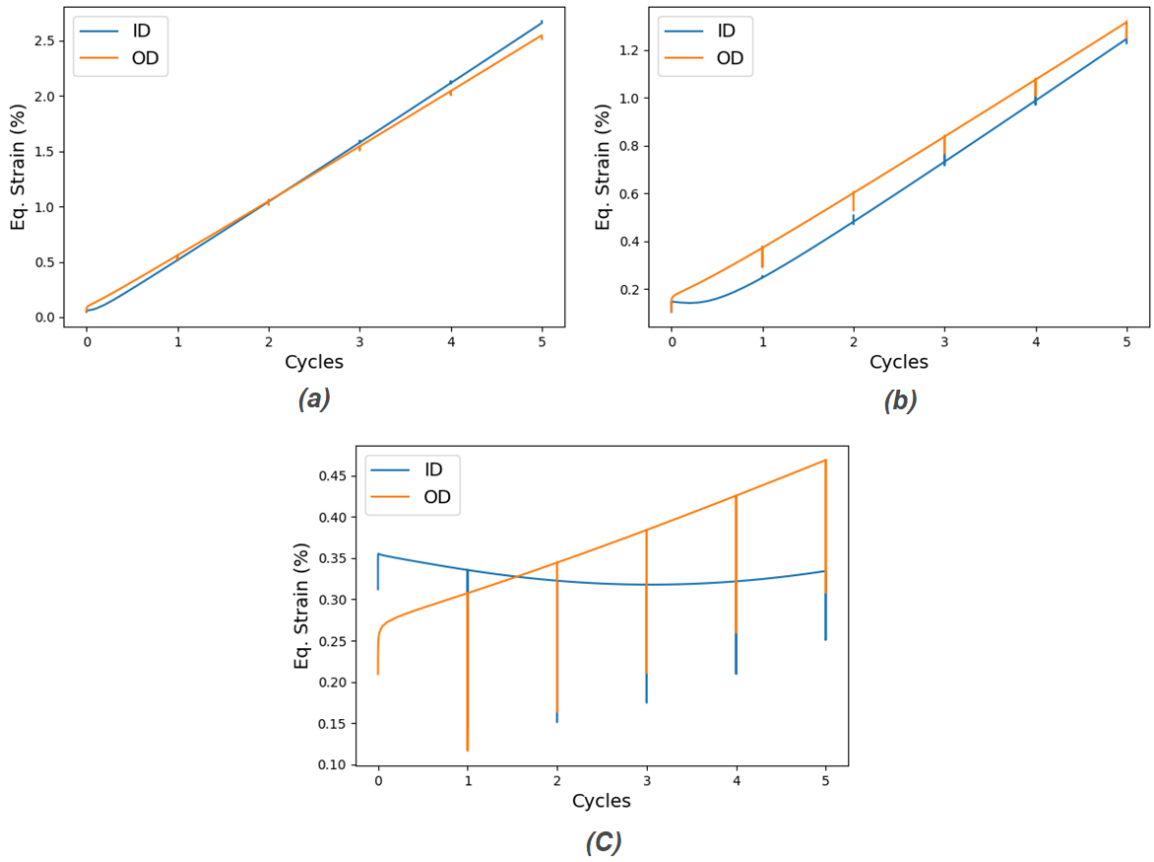

Figure 3.5: von Mises equivalent strain computed from inelastic analysis of the long cylinder at the inner and outer surfaces. Loading conditions are (a) $P = 0.5$, $\Delta T = 25$℃; (b) $P = 0.5$, $\Delta T = 50$℃; and (c) $P = 0.5$, $\Delta T = 100$℃ following the profiles showed in Figure 3.3.

The best estimate life and design life comparisons for the flat head vessel are provided in Table 3.5 and Table 3.6, respectively. Since the flat head vessel has geometric discontinuity, a bounding elastic follow up factor must be chosen for the EPP-SMT based life estimation. Instead of choosing a bounding value, however, the tables list EPP-SMT based life for different follow up factors. This allows assessing the EPP-SMT method with other methods for low and high values of the follow up factors.

The comparison between the two EPP-SMT approaches for the flat head vessel indicates that the classical approach estimates life shorter than the direct extrapolation approach when $\Delta T = 100$℃. For lower thermal load, the direct extrapolation approach estimates shorter creep-fatigue life of the flat head vessel. This can be explained by comparing the steady cyclic strain range for different loading conditions. As indicated by Figure 3.6, the steady cyclic strain range computed from EPP analysis is about 1.4 % at the knuckle for $P = 0.0\ MPa$, $\Delta T = 100$℃ loading. While the steady cyclic strain range at the knuckle is about 0.11% for $P = 0.0\ MPa$, $\Delta T = 25$℃ loading, as indicated by Figure 3.7. The 1.4% strain range falls into the high strain range regime where the classical approach bounds both approaches, as indicated by the plots in Figure 2.28 to Figure 2.30. For all the loading cases with $\Delta T = 50$℃ and $\Delta T = 25$℃, the strain range is always less than 0.3%

which falls in the regime where direct extrapolation approach predicts shorter creep-fatigue life than the classical approach.

Considering the lesser of the two estimated lives from EPP-SMT approaches and comparing that with other life estimation method indicates that EPP-SMT method with a follow up factor of 5 is comparable with the inelastic method, at least for $\Delta T \geq 50℃$ loading cases. This holds for both the best estimate life comparison, as listed in Table 3.5, and the design life comparison, as listed in Table 3.6. For all the loading cases with $\Delta T = 25℃$, the steady cyclic strain range from the EPP analysis is about 0.11% at the knuckle of the flat head vessel. This strain range again falls in the very low strain range regime where the use of direct extrapolation approach may be overly conservative. Similar conclusion was made from the long cylinder example above. A single SMT test data ($\Delta\varepsilon = 0.063\%$) in the similar strain range regime and with follow up factor of 3.5 also supports the over conservatism of the direct extrapolation approach in the very low strain range regime. See Figure 2.23 for the comparison between the test data and the EPP-SMT curves.

The following can be deduced from this comparative study:

1. The use of Equation 2.8, i.e. taking the lesser of the cycles to failure predicted by the two extrapolation approaches, is a reasonable approach for developing the EPP-SMT design curves. However, the direct extrapolation approach can be further improved by generating more data in the low strain range regime which in turn will improve the overall design curves by providing more accurate life predictions in the very low strain range regime.
2. The use of design factors of 2 on the strain range and 20 on cycles to failure for the EPP-SMT design curves is equivalent to the combined effect of all the design margins applied in the design by inelastic method including the factor $\left(\frac{1}{0.67}\right)$ applied to the stress.
3. Although additional analyses on different geometries are required before making final recommendation on the bounding follow up factor, the flat head vessel example shows EPP-SMT approach estimates life comparable to the design by inelastic analysis when a follow up factor of 5 is used for geometric discontinuities.
4. EPP-SMT design method is less over conservative compared to the design by elastic analysis.

Loading		Best estimate creep-fatigue life (cycles)							
		Inelastic analysis (no margin applied on stress relaxation history) + Average fatigue and average rupture stress	EPP analysis + nominal EPP-SMT curves based on						
			direct extrapolation			classical approach			
ΔT (°C)	P (MPa)		$q = 1$	$q = 3$	$q = 5$	$q = 1$	$q = 3$	$q = 5$
100	0	25	275	92	55	150	50	30
	0.1	26	283	94	57	156	52	31
	0.2	26	260	87	52	138	46	28
50	0	380	1368	456	274	3879	1293	776
	0.1	354	1532	511	306	6016	2005	1203
	0.2	346	1596	532	319	7085	2362	1417
25	0	4480	3481	1160	696	$1.1\text{x}10^7$	$3.5\text{x}10^6$	$2.1\text{x}10^6$
	0.1	3296	3829	1276	766	$2.6\text{x}10^7$	$8.8\text{x}10^6$	$5.3\text{x}10^6$
	0.2	2592	4076	1358	815	$4.6\text{x}10^7$	$1.5\text{x}10^7$	$9.1\text{x}10^6$

Table 3.5: Best estimate creep-fatigue life of the flat head vessel compared between inelastic analysis method and EPP-SMT method (with different follow up factors) for different loading conditions. The shaded cells indicate which of the two extrapolation approaches for EPP-SMT curves provides conservative estimation of the creep-fatigue life.

Loading		Creep-fatigue design life (cycles)							
		ASME design methods		EPP-SMT design method					
				direct extrapolation			classical approach		
ΔT (°C)	P (MPa)	Design by elastic analysis	Design by inelastic analysis	$q = 1$	$q = 3$	$q = 5$	$q = 1$	$q = 3$	$q = 5$
100	0	0	0	14	5	3	8	2	1
	0.1	0	1	14	5	3	8	2	1
	0.2	0	1	14	5	3	7	2	1
50	0	0	10	68	23	14	185	62	37
	0.1	0	10	77	26	15	301	100	66
	0.2	0	10	80	27	16	356	118	71
25	0	0	149	174	58	35	10410	3470	2082
	0.1	0	109	192	64	38	17742	5914	3548
	0.2	0	83	204	68	41	28382	9461	5676

Table 3.6: Creep-fatigue design life of the flat head vessel compared between current ASME design methods – design by elastic analysis and design by inelastic method – and the prospective EPP-SMT design method (with different follow up factors) for different loading conditions. The shaded cells indicate which of the two extrapolation approaches for EPP-SMT curves provides conservative estimation of the creep-fatigue life.

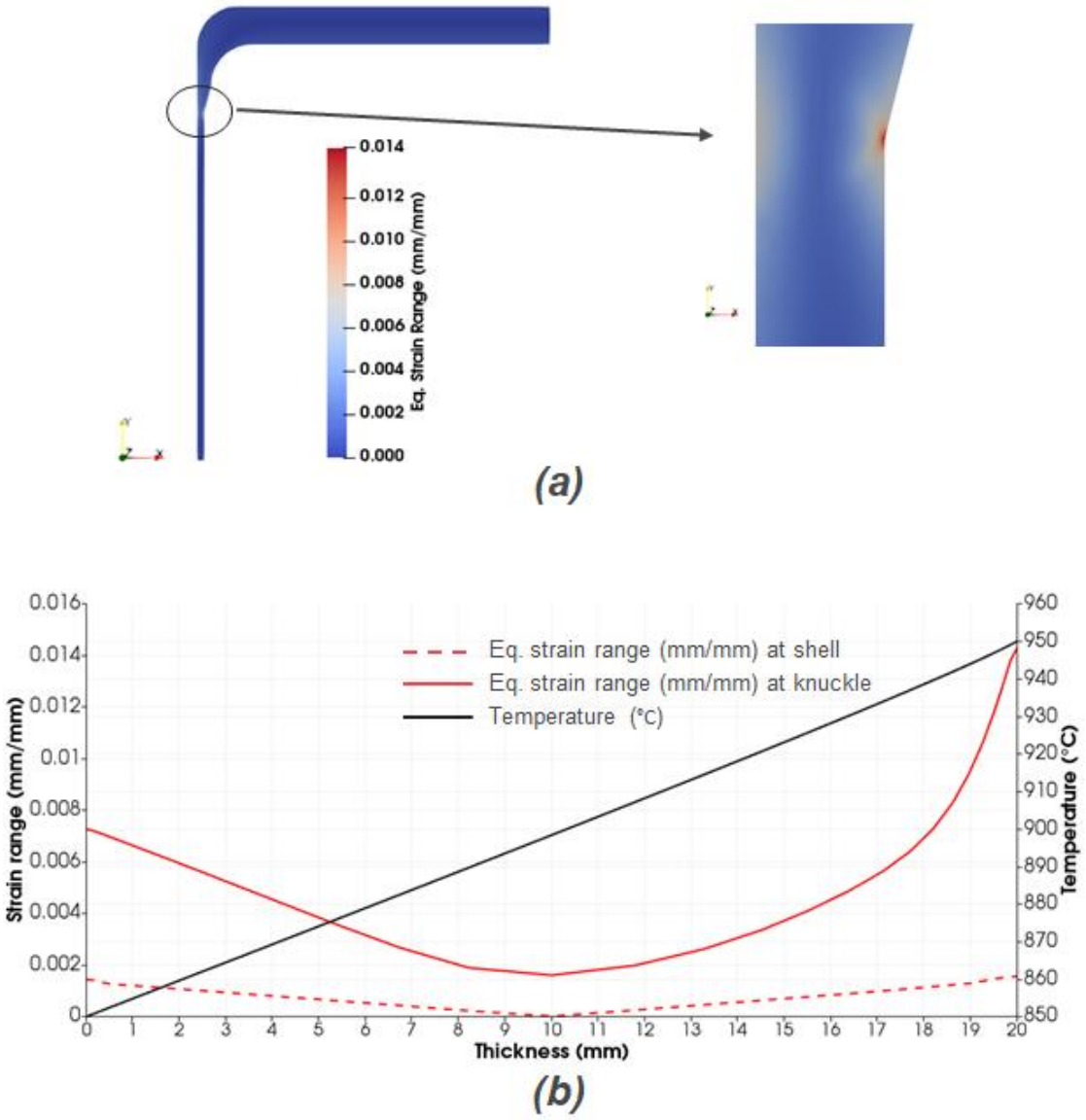

Figure 3.6: Through thickness steady cyclic equivalent strain range computed from EPP analysis of the flat head vessel. Loading condition is $P = 0.0, \Delta T = 100℃$ following the profiles showed in Figure 3.3.

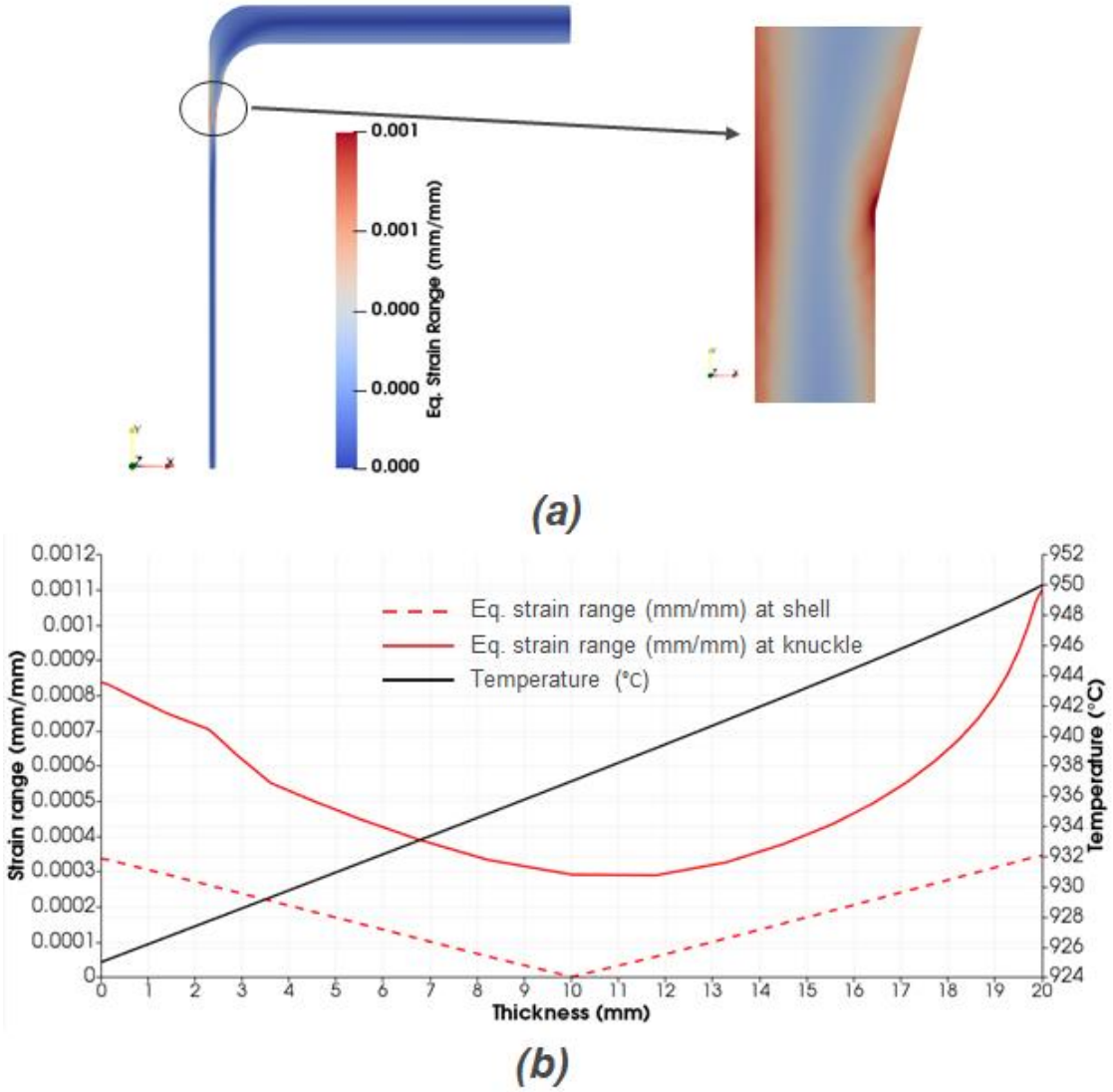

Figure 3.7: Through thickness steady cyclic equivalent strain range computed from EPP analysis of the flat head vessel. Loading condition is $P = 0.0$, $\Delta T = 25℃$ following the profiles showed in Figure 3.3.

4 Primary Load Effect

4.1 The effect of primary load on creep-fatigue life

The classical creep-fatigue test cycles a uniaxial specimen under strain control through a prescribed strain range. The test includes a hold at constant strain for some amount of time on either the tensile, compressive, or both ends of the cycle. The test continues until the specimen fails – either by breaking or until some predefined amount of load drop. As described elsewhere in this report, increasing the strain range on the specimen decreases its cyclic life [16]. Similarly, increasing the hold time tends to decrease the cyclic life of the sample. However, this effect saturates – eventually increasing the hold time at fixed strain only negligibly decreases the specimen life [14].

This report describes a third effect: elastic follow up [17]. In essence this is the difference between holding the specimen at fixed strain and holding the specimen through a spring with a finite stiffness. The standard creep-fatigue test has a follow up factor of $q = 1$, which indicates the hold period occurs through a spring with infinite stiffness, i.e. in pure strain control. Increasing this follow up factor equates to decreasing the spring stiffness. Increasing the follow up factor decreases the cyclic life of the specimen [18]. At least for experimentally-achievable values of the follow up factor this effect does not saturate, though the effect of increased follow up diminishes as the follow up factor increases (i.e. increasing the follow up factor from $q = 1$ to $q = 2$ results in a much greater decrease in life than increasing the factor from $q = 5$ to $q = 6$).

This chapter discusses a fourth effect, independent of strain range and hold time and only tangentially related to the follow up factor: the effect of primary load. Primary loads cause stresses in the component that creep stress relaxation cannot diminish. These stresses are necessary to maintain the specimen in equilibrium with the applied loads. Stresses caused by applied pressure are the classical example of a primary load. Secondary stresses are not required to maintain equilibrium with the applied loads. As such, at least for classical power-law creep materials, these stresses can relax to zero without affecting the balance of external forces on the component. A thermal stress is the classical example of a secondary stress. The load in a classical strain-controlled creep-fatigue experiment is entirely secondary.

In service components are nearly always loaded with both primary and secondary stresses. For example, a vessel might be loaded by internal pressure plus the thermal stress from a though-wall temperature gradient. For a component with fixed secondary load, increasing the primary load tends to decrease the component cyclic life [8]. The EPP-SMT design method must capture this "primary load effect."

Figure 4.1 shows the classical two bar model of superimposed primary and secondary load. The first bar is elastic and undergoes a fixed temperature cycle where the temperature in the bar increases, remains constant for some hold time, and decreases to the initial value. This induces secondary stress in the second bar. The second bar has an elastic-creep response. Conceptually, the temperature changes in the first bar occur instantaneously and creep in the second bar only occurs during the hold period. Both bars share an imposed primary load. In this example we consider the stress and strain history of the second bar (i.e. it is the test specimen). Figure 4.2 plots

the cyclic stress/strain from the 1st cycle and the stress relaxation history over 10 cycles of the second bar for different ratios between P (primary load) and $S = E_1 A_1 \Delta T \alpha_1$ (secondary load).

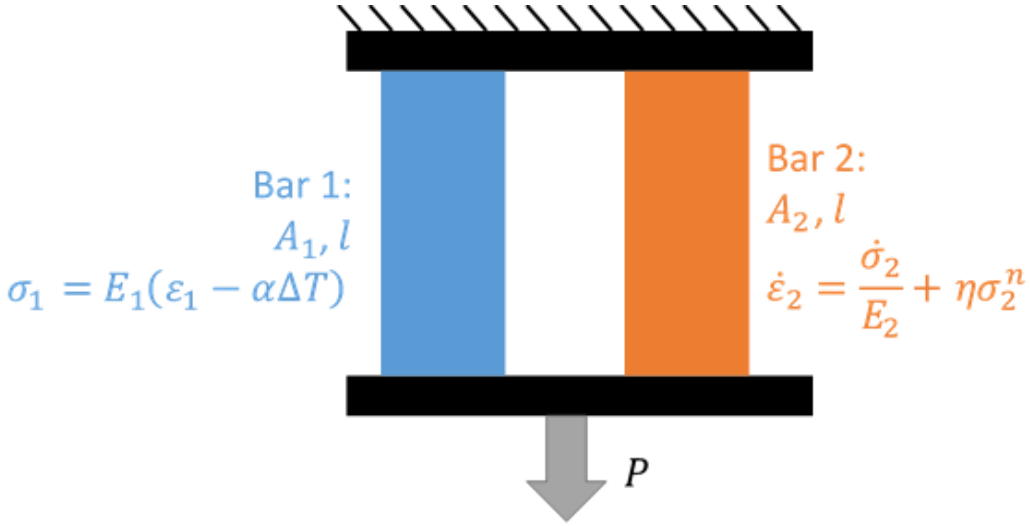

Figure 4.1: Standard two bar model of combined primary/cyclic secondary load.

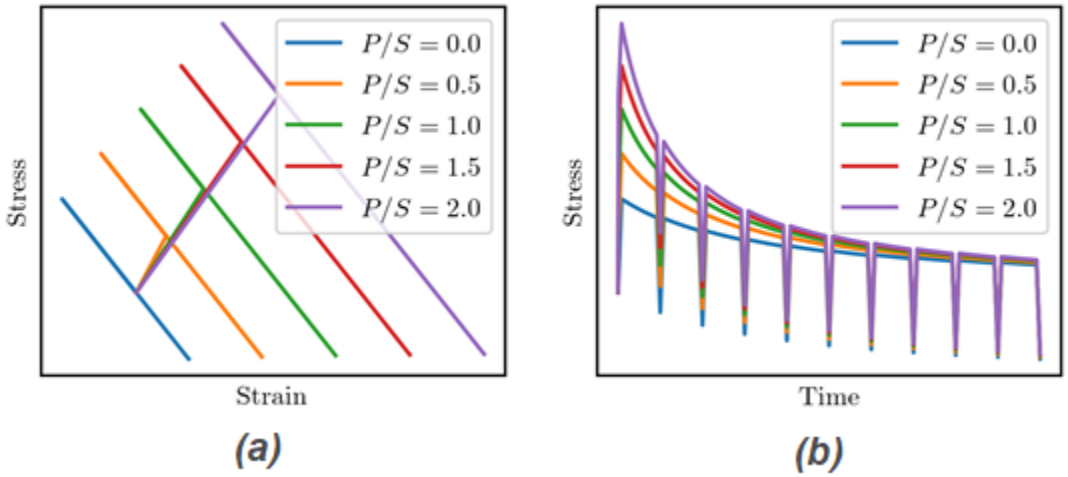

Figure 4.2: (a) Initial cycle strain/stress history of the two bar system for different P/S ratios. (b) Stress/time history for various P/S ratios.

Figure 4.3 summarizes the simulations in terms of the stress relaxation during the second cycle – the ratio between the final stress at the end of the hold and the initial stress at the start of the hold. As the ratio P/S increases the amount of stress relaxation in the test bar decreases. *The stress in the test bar cannot relax below the level required to maintain equilibrium with the applied primary load.* This reduction in the amount of stress relaxation is the classic explanation for the primary load effect. Higher primary load means the system experiences higher stresses for longer, when

compared to a specimen with a lower level of primary load. These higher stresses induce more creep damage, which diminishes the life of the component.

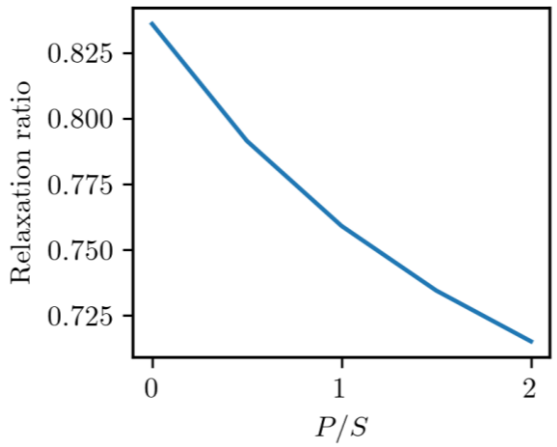

Figure 4.3: Ratio between the final stress and the initial stress during the relaxation hold in the second cycle.

There is a second, less-discussed effect of increasing the ratio between the primary and secondary stress. Figure 4.4 plots the total strain range over the second cycle during the simulations. Increasing the primary stress relative to a fixed secondary stress range increases the component strain range. The additional power-law creep caused by the higher overall stress in the second bar increases the strain range. However, rate independent plasticity could cause a similar effect.

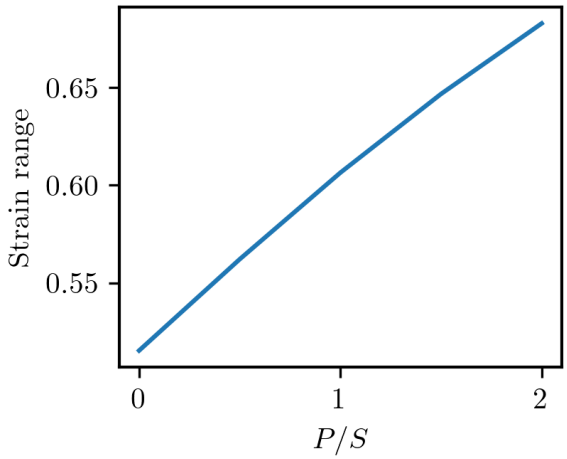

Figure 4.4: Strain range over the second load cycle as a function of P/S ratio.

4.2 Including the primary load effect in the EPP-SMT design method

4.2.1 Reference data

Test data combining primary and secondary loading on a sample could be used to validate a method for capturing the primary load effect in the new EPP-SMT method. The p-SMT (pressurized simplified model test) test, developed at Oak Ridge National Laboratory (ORNL) [7], provides a means for gathering this type of experimental data.

Figure 4.5 shows the p-SMT specimen. The specimen is a hollow uniaxial test article. Gas pressure in the inner cavity supplies the primary load. An applied displacement on the outer gauge supplies the secondary load. The method tunes the ratio of the inner and outer section lengths and areas to provide calibrated elastic follow up on the inner test bar. This type of testing can independently control all the factors influencing the specimen cyclic life: temperature, strain range (secondary load), hold time, follow up, and primary load.

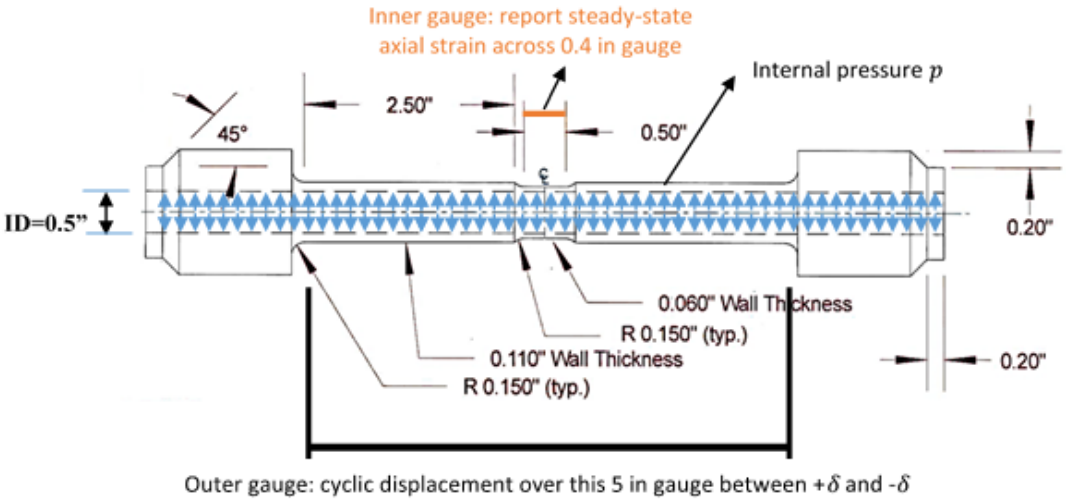

Figure 4.5: Diagram of the p-SMT specimen.

Table 4.1: p-SMT test database.Table 4.1 reproduces the results of a series of p-SMT tests at ORNL on Alloy 617 specimens. This particular test series keeps the outer gauge displacements (4.5 mils), the hold time (10 minutes, tensile), and the temperature (950°C) fixed and only changes the tube pressure. Table 4.1 demonstrates a moderate primary load effect – the cyclic life of the specimen decreases as the pressure increases.

Specimen	Pressure (psi)	Cycles to failure
INC617-P01	2	220
INC617-P02	200	220
INC617-P04	500	200
INC617-P03	750	150

Table 4.1: p-SMT test database.

In principle, a method for capturing the primary load effect could be tested against this data. However, that would require the EPP-SMT design curves (strain range versus cycles to failure, accounting for hold time and follow up effects) to be finalized. As described elsewhere in this report, the curves are not yet complete. As such, the following sections demonstrate the viability of primary load corrections to the method but do not provide final validation. Once the design curves finalized this dataset can be used to validate the primary load correction adopted by the final design procedure.

4.2.2 Bounding the primary load effect with the primary load limits

The EPP-SMT creep-fatigue check is one component of a larger set of design rules. The ASME design rules include primary load limits – limitations on the amount of primary load that can be applied to a component. The Section III, Division 5 rules express these limits as allowable stresses. The classical ASME approach compares these allowable stresses to a linearized and classified elastic stress analysis. A recently-developed alternate method applies EPP analysis to avoid stress classification [19].

These primary stress limits mean that properly-designed Division 5 components will limit, to some extent, the primary load effect on creep-fatigue life. However, the pressures in the p-SMT test series (Table 4.1) are all below the Division 5 primary load limit for the test specimen geometry. This suggests the primary load limits will not prevent the detrimental effect of the primary load on creep-fatigue life. However, the primary load limits will cap the primary load effect by limiting the primary load to a value well below the material rupture stress.

4.2.3 Capturing primary load with an increased strain range

As the primary load limits are insufficient to entirely prevent the primary load effect, the new EPP-SMT design method will need a mechanism for accounting for the decrease in cyclic life caused by the primary load. The current ASME design by elastic analysis creep-fatigue design approach limits stress relaxation to capture the primary load effect described in Figure 4.3. The current ASME time-fraction creep damage model is stress-based and so the reduction in stress relaxation is the logical way to capture the primary load effect.

However, Figure 4.4 demonstrates that there is a corresponding primary load effect on the strain range. Increasing the primary load increases the strain range in the test bar. This effect can only occur in component geometries with elastic follow up – i.e. when the material is not under pure

strain control. Under these conditions creep during the hold period induces strain in the material, increasing the overall strain range. The degree of elastic follow up controls this additional strain – larger follow up allows for a larger strain range increase.

Given that the EPP-SMT approach relies on the strain range, rather than the stress, this increased strain range is the natural way to capture the primary load effect. Table 4.2 demonstrates the EPP analysis method captures the increase in strain range with increasing primary load. This table lists results from an EPP analysis of the p-SMT specimens, applying the full EPP analysis method described in Chapter 5. The analysis correctly predicts an increase in the strain range with increasing primary load.

This increase in strain range may be sufficient to bound the primary load effect. Direct validation of this technique would require final EPP-SMT design curves for Alloy 617. As described elsewhere in the report, finalizing these design curves requires additional test data. However, Figure 4.6 suggests the increased strain range may be sufficient to capture the effect. This figure plots the EPP strain range versus the experimental cycles to failure for the p-SMT data. The data shows a threshold effect – very small primary loads increase the strain range but do not decrease the specimen life. However, at higher pressures the trend is approximately linear on a log-log scale, indicating a power law relation between the EPP strain range and the cycles to failure, including the primary load effect.

Specimen	Pressure (psi)	EPP strain range
INC617-P01	2	1.22%
INC617-P02	200	1.26%
INC617-P04	500	1.31%
INC617-P03	750	1.36%

Table 4.2: p-SMT EPP analysis results.

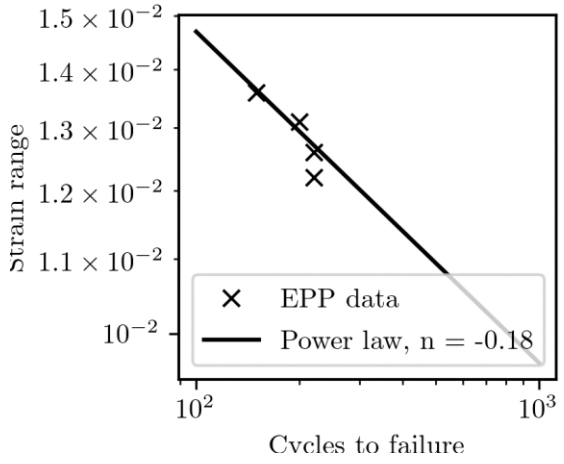

Figure 4.6: Log scale plot comparing the EPP strain range to the observed cycles to failure.

Chapter 2 notes that in the low cycle regime the SMT and creep-fatigue data, and therefore the EPP-SMT design curves, follows a power law of the type $\Delta\varepsilon \approx 1/N^a$. This suggests that the

primary load effect, as represented by an increased strain range, may capture the observed reduction in specimen life as both the primary load and base creep-fatigue and SMT data falls along a power law fit. Final validation of this approach will require the A617 design curves.

This approach would not capture the threshold effect in the p-SMT data – even a small primary load will lead to an increase in the strain range and a decrease in the allowable cycles. However, this is a conservative approximation. Future work could aim to capture the threshold either through additional testing or modeling.

4.2.4 Capturing primary load with a modified follow up factor

The British R5 Code contains a creep-fatigue design evaluation procedure based on strain via the ductility exhaustion approach to creep damage [20]. This design method then faces the same problem as the EPP-SMT method – capturing the primary load effect with a strain-based evaluation procedure. R5 addresses the primary load effect with a primary load modified follow up factor Z_p.[1]

Figure 4.7 outlines the idea of this "effective" follow up factor, which is calculated by fitting a standard elastic follow up relaxation profile to the composite stress history defined by the initial relaxation rate, the primary stress, which limits stress relaxation, and the cycle time.

The EPP-SMT rules include the effects of elastic follow up on creep fatigue life and can be tuned to different values of the follow up factor q. As such, the EPP-SMT approach could adopt a modified follow up factor to account for the primary load effect if the EPP strain range method fails to conservatively bound the p-SMT data using the final design curves.

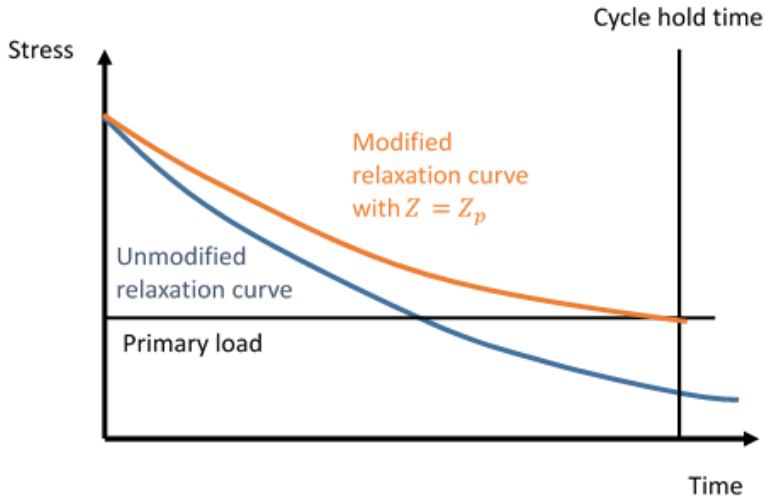

Figure 4.7: Schematic illustrating the primary load modified follow up factor.

[1] UK and European authors conventionally use Z for the follow up factor instead of q.

4.3 Recommendations

The EPP increased strain range approach has several advantages over using the primary load modified follow up factor:

1. There are no explicit changes to the design method to capture the primary load effect -- the EPP analysis itself directly captures the effect of the primary load through an increased strain range.

2. The follow up factor does not need to be a parameter in the final design method, meaning that EPP-SMT design curves for a fixed, bounding value of follow up can be provided, rather than a procedure for calculating damage as a function of follow up factor.

3. The increased strain range is an actual, physical effect. The modified follow up factor is an approximation designed to bound the effect of primary load on stress relaxation.

The initial version of the EPP-SMT design procedure described in Chapter 5 therefore accounts for the primary load effect using the EPP strain range approach. This method will need to be validated against the EPP-SMT design data once the Alloy 617 EPP-SMT design curves are finalized. The modified follow up factor approach is currently a backup plan – if the EPP strain range itself cannot bound the experimental primary load effect, the modified follow up factor could be used to capture the effect of primary load.

5 EPP-SMT design methodology

Several previous ART sponsored works [10][11][12] developed different elements of the EPP-SMT design methodology. The EPP-SMT design method for one type of loading cycle and for uniaxial deformation was proposed in [10]. This basic methodology was extended in [11] to account for multiaxial loading and the effect of combined load cycles. The definition of the pseudoyield stress for the EPP analysis to determine the stable cyclic strain range was developed in [12]. Finally, this current report develops the preliminary design charts for creep-fatigue damage evaluation in EPP-SMT design methodology in Chapter 2. Chapter 4 shows the EPP strain range should account for the primary load on creep-fatigue life although a validation against the finalized EPP-SMT design data is required. Finalizing the EPP-SMT design charts will require some additional creep-fatigue and SMT test data in the low strain range. The below provides step-by-step procedure of the initial version of the EPP-SMT design method.

Step 1 – Load definition

(i) Define all applicable loads and load cases per Section III, Division 5, HBB-3113.2, Service Loadings.

(ii) Make a histogram defining each Service Load as transient pressures, mechanical forces, and temperatures and/or thermal boundary conditions.

Step 2 – Composition cycle definition

(i) Generate one or more composite cycles by stitching together one or more of individual Service Loads into a single cycle. The composite cycle must be periodic – it must start and end at the same pressures, mechanical loads, and temperature and/or thermal boundary conditions. This may require postulating new loads that are not defined in the Design Specification. The number of composite cycles and the ordering of each individual Service Load within a composite cycle should be guided by any information about the expected ordering of Service Loads in actual operation. In the absence of such information, distributing transients uniformly throughout the component design life typically produces a reasonable composite cycle

(ii) Assign a number of cycle repetitions of each individual loading within the composite cycle, and refer this number to as the loading weight, W_i^j with i being the cycle type and j being the composite cycle type. This information is metadata and does not imply that the load condition is actually repeated the indicated number of times, either within the composite cycle or in terms of total analysis repetitions of the composite cycle. If any, the fictitious loads to enforce periodicity in Step 2 – (i) should be assigned a zero weight. In assigning these weights the total number of repetitions assigned to a region representing a particular Service Load in all composite cycles must sum to the total repetitions of that Service Load in the Design Specification, i.e. $\sum_j^{n_j} W_i^j = W_i$, where n_j is the total number of composite cycles and W_i is the total number of repetitions of cycle i in Design Specification.

Step 3 – Numerical model

Develop a numerical model of the component, including all relevant geometric characteristics. The model used for the analysis shall be selected to accurately represent the component geometry, boundary conditions, and applied loads. The model must also be accurate for small details, such as small holes, fillets, corner radii, and other stress risers. The local temperature history shall be determined from a thermal transient analysis based on the thermal boundary conditions determined from the loading conditions defined in Step 2.

Step 4 – Elastic-perfectly plastic (EPP) analysis

(i) Determine the cycle period, t^j corresponding to each composite cycle defined in Step 2. This cycle period is the total time of the Service Loads assigned to each individual composite cycle, accounting only for the individual Service Load within the composite cycle and not the product of this time and the weight factor. Fictitious loads used to enforce the periodicity shall be assigned zero time in this calculation.

(ii) For each composite cycle determine the temperature dependent pseudoyield stress, $S_\varepsilon^j(T)$ from the isochronous stress-strain curves in Code Cases: Nuclear Components N-898 for a 0.2% offset in strain from the elastic slope at temperature, T and for time t^j.

(iii) Perform a small strain, EPP cyclic analysis for each composite cycle with the temperature dependent pseudoyield stress $S_\varepsilon^j(T)$. Other temperature-dependent mechanical properties required are the Section II Young's modulus, Poisson's ratio and coefficient of thermal expansion coefficient. The assessment temperature shall be taken as the local instantaneous temperature at every location in the numerical model of the component. The EPP analysis may neglect hold times and use arbitrary loading rates, as the analysis method is rate independent

(iv) If elastic or plastic shakedown occurs in the EPP analysis, that is, cycles with either eventual elastic behavior everywhere or constant cyclic elastic-plastic behavior without ratcheting everywhere, proceed to Step 5. If a shakedown does not occur, the structure does not pass the creep-fatigue damage check for the applied loading condition.

Step 5 – Creep-fatigue damage evaluation

(i) Determine all the total, elastic plus plastic, strain components $(\varepsilon_x, \varepsilon_y, \varepsilon_z, \gamma_{xy}, \gamma_{yz}, \gamma_{zx})$ for each composite cycle at each point of interest from the shakedown analysis performed in (iii) of Step – 4 above.

(ii) Calculate an effective strain range for each region in the composite cycle. Calculating an effective strain range requires two points in time: a reference point and the current time under consideration. When defining the effective strain range for a particular region, the designer should find the maximum effective strain range for any reference point in the cycle, o but only current times, k in the region under consideration, following the substeps below:

a. Calculate the history of change in strain components by subtracting the value at the time, o from the corresponding components at each point in time, k of the region under consideration.

$$\Delta\varepsilon_{x,k} = \varepsilon_{x,k} - \varepsilon_{x,o}\ ; \quad \Delta\varepsilon_{y,k} = \varepsilon_{y,k} - \varepsilon_{y,o}; \quad \text{etc.}$$

b. Calculate the equivalent strain range for each point in time, k of the region under consideration as:

$$\Delta\varepsilon_{equiv}.,k = \frac{\sqrt{2}}{3}\Big[\left(\Delta\varepsilon_{x,k} - \Delta\varepsilon_{y,k}\right)^2 + \left(\Delta\varepsilon_{y,k} - \Delta\varepsilon_{z,k}\right)^2 + \left(\Delta\varepsilon_{z,k} - \Delta\varepsilon_{x,k}\right)^2 + \frac{3}{2}\left(\Delta\gamma_{xy,k}^2 + \Delta\gamma_{yz,k}^2 + \Delta\gamma_{zx,k}^2\right)\Big]^{\frac{1}{2}}$$

c. Define the effective strain range as the maximum of the above calculated equivalent strain ranges, $\Delta\varepsilon_{equiv}.,k$.

(iii) Record the effective strain range, $\Delta\varepsilon_{eff.,i}^{j}.$ calculated in (ii)-c for each region of each composite cycle. Determine a corresponding Service Load time, $t_i^j.$ which is the total time at the particular Service Load conditions, including time during loading transients. Determine the maximum metal temperature, T_i^j over that region of the composite cycle. Using the strain range $\Delta\varepsilon_{eff.,i}^{j}$, time t_i^j, and temperature T_i^j determine an allowable number of design repetitions, N_i^j from the EPP-SMT design charts.

(iv) Calculate the use fraction of the component at each material point using:

$$D = \sum_{j=1}^{n_j}\sum_{i=1}^{n_i}\frac{W_i^j}{N_i^j}$$

where the sum proceeds over all the regions, i of all the composite cycles, j.

(v) The structure passes the creep-fatigue design check if $D \leq 1$ for all points in the component.

6 Conclusions

6.1 Summary and conclusions

Development of the EPP-SMT design charts requires extrapolating results of creep-fatigue and SMT tests at high strain range regime and with short hold times to the low strain range regime and long holds. The report compares two such extrapolation approaches – direct extrapolation and classical approach – developed in [10]. Direct comparison with test data indicates that both approaches reasonably capture experimental results in the high strain range regime. The comparison in the low strain range regime, although based on a single SMT test data, indicates that the classical approach over predicts the cyclic life by several orders of magnitude. In contrast, the direct extrapolation approach under predicts the test result, although the difference is much less compared to that for the classical approach. Therefore, this work takes a conservative approach in constructing the preliminary design charts, that is, use the lesser of the cycles to failure predicted by the two extrapolation approaches. Finalizing the design charts requires additional test data in the low strain range regime.

The report compares the EPP-SMT method with other design methods in the ASME Code through evaluating creep-fatigue life of two different structures subjected to different thermal and pressure loadings. Results from this comparative analysis indicate that the conservative approach of constructing design charts is a reasonable approach considering the lack of data in the low strain range regime. However, those results also indicate that the extrapolation approach can be improved with additional data which can further reduce the over conservatism in the creep-fatigue damage evaluation. Another important finding from this comparative analysis is the use of design factors 2 on the strain range and 20 on cycles to failure for the EPP-SMT design charts is equivalent to the combined effect of all the design margins applied in the design by inelastic analysis method.

The report also describes several approaches for including the primary load effect in the EPP-SMT design method. However, the simple approach of using the EPP increased strain range combined with a bounding follow up factor for the EPP-SMT design charts offers several advantages over other approaches, most importantly, it does not require any explicit change in the initial design method described in this report.

6.2 Future work

Chapter 5 of this report provides the initial version of the EPP-SMT design method. Finalizing the design method requires:

1. Additional creep-fatigue and/or SMT test data in the low strain regime for finalizing the extrapolation procedure used in constructing the design charts. The hold time for these tests should be sufficiently long enough for the stress to relax during the hold but short enough for the test to complete in reasonable time. The stress relaxation profile from isochronous stress-strain curves can help decide the hold time for these tests.
2. Finalizing a bounding value of the follow up factor to be used for constructing the design charts. We currently envision basing the design charts off a representative follow up factor, likely in the range of $q = 2$ to $q = 5$. The exact value could be determined by examining typical reactor structural components with a full inelastic analysis.

3. Construct the EPP-SMT design charts at temperatures lower than 800°C but higher than the negligible creep temperature for Alloy 617. Since no creep-fatigue or SMT test data are available for these temperatures, an approach could be extrapolating the shift parameters, p and D in Equation 2.2, from higher temperatures to lower temperatures and using those parameters to construct the design charts. Then, verify the design charts through a comparative analysis with other design methods for different sample structures.

Oak Ridge National Laboratory (ORNL) will be generating additional creep-fatigue and SMT test data for Alloy 617 in the low strain range regime. With these additional test data, the future work will focus on resolving the issues above to complete the design method and afterwards begin the ASME Code approval process for a new EPP-SMT Code Case.

Acknowledgements

The research was sponsored by the U.S. Department of Energy, under Contract No. DEAC02-06CH11357 with Argonne National Laboratory, managed and operated by UChicago Argonne LLC. Programmatic direction was provided by the Office of Nuclear Reactor Deployment of the Office of Nuclear Energy. The authors gratefully acknowledge the support provided by Sue Lesica, Federal Manager, Advanced Materials, Advanced Reactor Technologies (ART) Program, Diana Li, Federal Manager, ART Gas-Cooled Reactors (GCR) Campaign, and Gerhard Strydom of Idaho National Laboratory (INL), National Technical Director, ART GCR Campaign.

Bibliography

[1] American Society of Mechanical Engineers. Section III, Division 5. In *ASME Boiler and Pressure Vessel Code*. 2019.

[2] American Society of Mechanical Engineers. Code Case N-862. In *ASME Boiler and Pressure Vessel Code*. 2017.

[3] Jetter, R. I. (1998). An Alternate Approach to Evaluation of Creep-Fatigue Damage for High Temperature Structural Design Criteria. *ASME-PUBLICATIONS-PVP*, *365*, 199-206.

[4] Messner, M. C., Sham, T. L., Wang, Y., & Jetter, R. I. (2018). *Evaluation of methods to determine strain ranges for use in SMT design curves* (No. ANL-ART-138). Argonne National Lab.(ANL), Argonne, IL (United States).

[5] Wang, Y., Messner, M. C., Sham, T. L. (2018). *Report on the FY18 Uniaxial Material Model Testing and Key Feature Test Articles Testing of Grade 91* (No. ORNL/TM-2018/885). Oak Ridge National Lab.(ORNL), Oak Ridge, TN (United States).

[6] Wang, Y., Jetter, R. I., Messner, M. C., Sham, T. L. (2018). *Report on FY18 Testing Results in Support of Integrated EPP-SMT Design Methods Development* (No. ORNL/TM-2018/887). Oak Ridge National Lab.(ORNL), Oak Ridge, TN (United States).

[7] Wang, Y., Jetter, R. I., Messner, M. C., & Sham, S. (2019). *Report on FY19 Testing in Support of Integrated EPP-SMT Design Methods Development* (No. ORNL/TM-2019/1224). Oak Ridge National Lab.(ORNL), Oak Ridge, TN (United States).

[8] Wang, Y., Jetter, R. I., & Sham, T. L. (2016). FY16 Progress Report on Test Results In Support Of Integrated EPP and SMT Design Methods Development. *ORNL/TM-2016/330, Oak Ridge National Laboratory, Oak Ridge, TN*.

[9] Wang, Y., Jetter, R. I., Krishnan, K., & Sham, T. L. (2013). Progress Report on Creep-Fatigue Design Method Development Based on SMT Approach for Alloy 617. *ORNL/TM-2013/349, Oak Ridge National Laboratory, Oak Ridge, TN*.

[10] Messner, M. C., Jetter, R. I., Wang, Y., & Sham, T. L. (2019). *Initial Development of an Improved Creep-Fatigue Design Method that Avoids the Separate Evaluation of Creep and Fatigue Damage and Eliminates the Requirement for Stress Classification* (No. ANL-ART-168). Argonne National Lab.(ANL), Argonne, IL (United States).

[11] Messner, M. C., & Sham, T. L. (2019). *Development of a multiaxial deformation measure and creep-fatigue damage summation for multiple load cycle types in support of an improved creep-fatigue design method* (No. ANL-ART-164). Argonne National Lab.(ANL), Argonne, IL (United States).

[12] Messner, M. C., Sham, T. L., Wang, Y., & Jetter, R. I. (2018). *Evaluation of methods to determine strain ranges for use in SMT design curves* (No. ANL-ART-138). Argonne National Lab.(ANL), Argonne, IL (United States).

[13] Huddleston, R. L. (1985). An improved multiaxial creep-rupture strength criterion.

[14] Coffin, L. F. (1976). The Concept of Frequency Separation Methods in Life Prediction for Time-Dependent Fatigue. In *ASME-MPC Symposium on Creep-Fatigue Interaction (MPC-3)* (pp. 346-363).

[15] American Society of Mechanical Engineers. Code Case N-898. In *ASME Boiler and Pressure Vessel Code*. 2019.

[16] Goswami, T. (2004). Development of generic creep-fatigue life prediction models. Materials and Design, 25(4), 277–288.

[17] Boyle, J. T., & Nakamura, K. (1987). The assessment of elastic follow-up in high temperature piping systems—overall survey and theoretical aspects. *International journal of pressure vessels and piping*, *29*(3), 167-194.

[18] Wang, Y., Li, T., Sham, T. L., & Jetter, R. I. (2013). Evaluation of Creep-Fatigue Damage Based on Simplified Model Test Approach. In *Pressure Vessels and Piping Conference* (Vol. 55638, p. V01AT01A044). American Society of Mechanical Engineers.

[19] Messner, M. C., & Sham, T. L. (2020). *Initial development and verification of a primary load design method based on elastic-perfectly plastic analysis* (No. ANL-ART-201). Argonne National Lab.(ANL), Argonne, IL (United States).

[20] British Energy. (2015). R5: Assessment Procedure for the High Temperature Response of Structures.

[21] Kocks, U. F. (2001). Realistic constitutive relations for metal plasticity. Materials Science and Engineering: A, 317(1-2), 181-187.

[22] Estrin, Y., & Mecking, H. (1984). A unified phenomenological description of work hardening and creep based on one-parameter models. Acta metallurgica, 32(1), 57-70.

[23] Wang, Y., Jetter, B., Messner, M. C., & Sham, T. L. (2019). Development of Simplified Model Test Methods for Creep-Fatigue Evaluation. In *Pressure Vessels and Piping Conference* (Vol. 58929, p. V001T01A065). American Society of Mechanical Engineers.

[24] Messner, M. C., Jetter, B., & Sham, T. L. (2019). A Method for Directly Assessing Elastic Follow Up in 3D Finite Element Calculations. In *Pressure Vessels and Piping Conference* (Vol. 58929, p. V001T01A064). American Society of Mechanical Engineers.

[25] Wang, Y., Jetter, R. I., Messner, M. C., Mohanty, S., & Sham, T. L. (2017). Combined Load and Displacement Controlled Testing to Support Development of Simplified Component Design Rules for Elevated Temperature Service. In *Pressure Vessels and Piping Conference* (Vol. 57915, p. V01BT01A016). American Society of Mechanical Engineers.

[26] Sham, T. L., Jetter, R. I., & Wang, Y. (2016). Elevated temperature cyclic service evaluation based on elastic-perfectly plastic analysis and integrated creep-fatigue damage. In *Pressure Vessels and Piping Conference* (Vol. 50367, p. V01BT01A022). American Society of Mechanical Engineers.

A Alloy 617 test database

The following tables list database for the fatigue and creep-fatigue tests at 800°C, 850°C, and 950°C and SMT tests at 950°C on Alloy 617. The strain ranges are the controlled strain range for the fatigue and creep-fatigue tests ($q = 1$) and the EPP strain range for the SMT tests ($q > 1$).

T (°C)	*Δε (%)*	*N*
800	0.3	29680
800	1	690
800	1	890
850	0.3	10495
850	0.3	8904
850	0.3	10631
850	0.6	1712
850	0.6	1584
850	0.6	1423
850	0.6	2,139
850	0.6	1394
850	0.6	1633
850	0.6	1886
850	1	821
850	1	850
850	1	813
950	0.3	9641
950	0.3	5867
950	0.3	9054
950	0.3	7133
950	0.3	8333
950	0.4	2378
950	0.4	2326
950	0.6	1722
950	0.6	1390
950	0.6	1480
950	0.6	1342
950	0.6	1295
950	0.6	1432
950	0.6	1266
950	0.6	1085
950	0.6	1498
950	0.6	1254
950	0.6	1233
950	0.6	1229
950	0.6	1506
950	1	963
950	1	972
950	1	916
950	1	897

Table A.1 Fatigue test database for Alloy 617 at 800°C, 850°C, and 950°C.

T (°C)	*Δε (%)*	t_h *(min)*	*Hold type*	*N*
800	0.3	0.3	T	8160
800	0.3	1	T	8370
800	0.3	1	T	4760
800	0.3	10	T	3960
800	0.3	10	T	3500
800	1	1	T	485
800	1	1	T	440
800	1	3	T	546
800	1	10	T	580
800	1	10	T	390
850	0.3	3	T	1944
850	0.3	3	T	2547
850	0.3	10	T	1475
850	0.3	10	T	1750
850	0.3	10	T	2104
850	0.3	30	T	1200
850	0.3	30	T	1255
850	0.3	60	T	1025
850	0.3	120	T	1200
850	0.6	1	T	1182
850	0.6	1	T	994
850	0.6	1	T	1008
850	0.6	1	T	1280
850	0.6	1	T	1434
850	0.6	1	T	1192
850	0.6	1	T	1565
850	0.6	1	T	1390
850	1	3	T	544
850	1	3	T	660
850	1	10	T	487
850	1	10	T	548
850	1	30	T	371
850	1	30	T	453
850	1	120	T	148
850	1	120	T	311
850	1	240	T	114
850	1	240	T	155
950	0.3	0.033	T	4083
950	0.3	0.033	T	3538
950	0.3	3	T	4486
950	0.3	3	T	3984
950	0.3	3	T	2485
950	0.3	10	T	4096
950	0.3	10	T	4430
950	0.3	10	T	2623
950	0.3	10	T	4361
950	0.3	30	T	4832
950	0.3	30	T	4650
950	0.3	30	T	2653
950	0.3	3	C	4373
950	0.3	3	T & C	1310
950	0.3	12	T & C	1159
950	0.4	1	T	1680

T (°C)	*Δε (%)*	t_h *(min)*	*Hold type*	*N*
950	0.4	1	T	1768
950	0.6	1	T	1085
950	0.6	1	T	953
950	0.6	1	T	975
950	0.6	1	T	904
950	0.6	1	T	1048
950	0.6	3	T	950
950	0.6	3	T	922
950	0.6	10	T	686
950	0.6	10	T	634
950	0.6	10	T	547
950	0.6	30	T	661
950	0.6	30	T	1110
950	0.6	30	T	525
950	0.6	1	T	826
950	0.6	1	T	986
950	0.6	1	T	1046
950	0.6	1	T	1054
950	0.6	1	T	937
950	1	0.033	T	820
950	1	0.033	T	790
950	1	3	T	376
950	1	3	T	465
950	1	3	T	472
950	1	10	T	308
950	1	10	T	391
950	1	10	T	427
950	1	10	T	430
950	1	30	T	322
950	1	30	T	364
950	1	30	T	334
950	1	150	T	386

Table A.2 Creep-fatigue test database for Alloy 617 at 800°C, 850°C, and 950°C. Hold directions are given with codes indicating a tensile hold (T), compressive hold (C), or both (T/C).

$\Delta\varepsilon$ (%)	q	t_h (min)	Hold type	N
0.206126	2.7	10	T	270
0.206126	2.7	10	T	940
0.206126	2.7	10	T	950
0.368072	2.7	10	T	370
0.368072	2.7	10	T	350
0.368072	2.7	10	T	1000
0.379492	2.7	20	T&C	400
0.063094	3.5	3	T	10660
0.254669	3.5	10	T	1000
0.254669	3.5	10	T	900
0.254669	3.5	10	T	1100
0.254669	3.5	10	C	1200
0.272193	3.5	20	T&C	1050
0.32547	3.5	0	N	1600
0.480447	3.5	10	T	460
0.480447	3.5	10	T	450
0.480447	3.5	10	T	950
0.480447	3.5	10	C	600
0.49797	3.5	20	T&C	600
0.507171	3.5	30	T	230
0.558454	3.5	600	T	150

Table A.3 SMT test database for Alloy 617 at 950°C. Hold directions are given in the table with codes indicating a tensile hold (T), compressive hold (C), both (T/C), or no hold.

Applied Materials Division
Argonne National Laboratory
9700 South Cass Avenue, Bldg. 212
Argonne, IL 60439

www.anl.gov